# The Eocene-Oligocene palynological record from the Xining Basin (Tibetan Plateau, NW China) as evidence for Asian palaeoenvironments and regional change

**MSc. Thesis**
**Julia Straathof (0302090)**
**February 2010**
**Utrecht University**

**Supervisors:**

**Dr. G. Dupont-Nivet (Paleomagnetic Laboratory "Fort Hoofddijk", Faculty of Geosciences, Utrecht University)**
**Dr. C. Hoorn (Institute for Biodiversity and Ecosystem Dynamics, University of Amsterdam)**

## Abstract

The Eocene–Oligocene transition (EOT) is marked by global cooling trend that coincided with rapid growth of the Antarctic ice sheet and a drop in atmospheric carbon dioxide levels. This trend is particularly well registered in the oceanographic record, but complete continental sequences comprising this transition are sparse. Even rarer are palynological records of this period of climatic change.

Here we report on a palynological study of playa lake deposits situated in the Xining Sub-basin (Tibetan Plateau, NW China). In this basin the EOT was identified by a regional lithological change in the red bed / gypsum alternation and was precisely dated through palaeomagnetostratigraphy. This sedimentary sequence also proved rich in pollen.

High abundances (and many varieties) of *Ephedra* and *Nitraria,* taxa typical for arid vegetation types, characterize the palynology of the Xining Sub-basin. Subtle fluctuations of these taxa throughout the sequence suggest that the local vegetation alternated from desert type (*Ephedra* dominated) to -slightly more humid- steppe type (*Nitraria* dominated) and back. The palynological results of the studied section fit well in the wider Chinese context during the EOT when a broad arid belt crossed China from East to West. By Neogene times the arid zone was restricted to NW China (Sun & Wang, 2005) and palynological assemblages were no longer *Ephedra* and *Nitraria* dominated.

A surprising increase in high altitude distal pollen influx (Pinaceae) occurs just below the E-O boundary and is considered to be evidence for climatic cooling and/or increased topography in the Tibetan Plateau during the Late Eocene.

# Content

# 1. Introduction

Palynological analysis of fossil pollen assemblages is a powerful method for reconstructing palaeoenvironmental conditions. When combined with high resolution age control it enables to decipher tectonic vs. climatic forcing of palaeoenvironmental conditions. Here we apply palynological methods to a well dated continental lacustrine stratigraphy from the Xining Basin (NW China) that holds the record of both Tibetan plateau uplift (Dupont-Nivet et al., 2008) and a major global climate event, namely, the Eocene-Oligocene transition (Dupont-Nivet et al., 2007).

## 1.1 Tibetan Plateau uplift

The youngest and most spectacular of all the continent-continent collision belts on Earth is the Himalayan-Tibetan orogen, encompassing the Himalaya and Karakorum ranges in the south and the enormous Tibetan plateau to the north. This orogenic system was created by the Indo-Asian collision and is part of the greater Himalayan-Alpine system that extends from the Mediterranean Sea in the west to the Sumatra arc of Indonesia in the east over a distance of more than 7000 km (Yin and Harrison, 2000).

Timing of the initiation of uplift and deformation across the Tibetan Plateau is still poorly constrained and therefore one of the most studied and debated geological topics. For a long time it was thought that the initial onset of the Tibetan Plateau uplift only started in the Miocene. Nowadays more and more data prove that this uplift initiated ca. 50 Ma. However, this has been recently challenged by proposition of a 35 Ma age for the collision (Aitchinson et al., 2007).

According to Royden et al. (2008) the development of high topography and thickened crust in the Tibetan region may have began already before continental collision, during subduction of the Tethys Ocean beneath Eurasia. Crustal thickening took place in what is now central Tibet during Early Cretaceous. By the Late Cretaceous the southern and central plateau was elevated above sea level, although marine deposits in northern Tibet suggest low areas during Cretaceous-early Tertiary time (Yin and Harrison, 2000). After the Indo-Asia collision, intracontinental convergence and deformation continued across Tibet. During the Early Cenozoic the crust was shortened in western and central Tibet and in Eocene-Oligocene times the southern and central part of the Tibetan Plateau were

uplifted to high elevations (Royden et al., 2008). Yin and Harrison (2000) state that the construction of the Cenozoic Tibetan Plateau began more or less synchronously in the Eocene (50–40 Ma) in the Tethyan Himalaya in the south, and in the Kunlun Shan and the Qilian Shan some 1000–1400 km to the north. Wang et al. (2008a) also hypothesize that central Tibet was uplifted at Paleogene times, but suggest a different model for the tectonics. Firstly, the central plateau was uplifted, forming a high proto-Tibetan Plateau. The plateau expanded as a result of the continued collision of India with Asia. To the south, the Himalaya rose during the Neogene, while to the north, the Qilian Shan uplifted. Tapponnier et al. (2001) also suggest that the growth of the plateau occurred stepwise. The Plateau rose in three steps from south to north, at each step, high plains formed by filling in internally drained intermontane basins. $^{40}Ar/^{39}Ar$ and zircon U–Pb dating of lavas of the central-western Qiangtang Block proves that the elevation of the central Tibetan Plateau indeed began in Paleogene times, as early as 45–38 Ma ago (Wang et al., 2008b). Also oxygen-isotope-based estimates of palaeo-altitude from late Eocene–Oligocene formations in the Lunpola Basin in central Tibet indicate that the centre of the plateau has been characterized by elevations in excess of 4 km since 35 ± 5Myr ago (Rowley and Currie, 2006).

## 1.2 Tibetan uplift and climate change

The interaction between the lithospheric deformation and the atmosphere makes the Himalayan-Tibetan orogen of even greater interest.

Climate models show that uplift of the Tibetan Plateau and the redistribution of land and sea, associated with the continent-continent collision of India and Asia, caused continental aridification and intensification of the monsoons (Ramstein et al., 1997). As a result, palaeoenvironmental records have invariably associated Tibetan uplift to evidence for aridification north of the Tibetan Plateau and monsoon intensification to the south (Sun and Wang, 2005). However, it has been recently demonstrated from the stratigraphy studied here, that Asian palaeoenvironment is also governed by global climate changes. Using high resolution chronostratigraphy aridification recorded in the studied stratigraphy is closely correlated to the Eocene-Oligocene transition; an abrupt cooling event at 34 Ma associated to the glaciation of Antarctica (Dupont-Nivet et al., 2007). Our study will focus on the palynology of this well-dated stratigraphy recording the period leading to the Eocene-Oligocene transition.

It has been further hypothesized that the Tibetan Plateau uplift may also be the cause of the global Cenozoic global cooling from greenhouse to icehouse conditions (Ruddiman, 2001). This gradual global cooling from ca. 50 Ma to today, culminated at 34 Ma with the Eocene-Oligocene transition.

The uplift of the Himalaya and the Tibetan Plateau resulted in large exposure of fresh rock on steep slopes. The steep slopes received intense rainfall generated by the monsoon rains, which resulted in rapid chemical weathering. Weathering of silicate rocks by hydrolysis is the main way that $CO_2$ is pulled out of the atmosphere, and subsequent consumption of atmospheric $CO_2$ leads to global cooling. An index to determine global chemical weathering is the ratio of two isotopes of the element strontium. Trace amounts of the element are incorporated into shells of plankton (Ruddiman, 2001). Throughout the Cenozoic, seawater 87Sr/86Sr shows an increase, beginning after ca. 40 Ma, with the greatest change at ca. 38 Ma. This study will focus on a pollen record that suggests evidence for Tibetan uplift at around this time and has led to attribute this 87Sr/86Sr

increase to erosion of the Himalayan-Tibetan orogen uplifting at this time and may have led to threshold conditions for the Eocene Oligocene transition at 34 Ma (Dupont-Nivet et al., 2008) (Garzione, 2008).

## 1.3 Aim of study

Dupont-Nivet et al. (2008) presented initial results on palynological assemblages recovered from sediments from the Xining sub-basin, and reported appearances of high-altitude vegetation around 38 Ma (later changed to 36 Ma by new age control). This was interpreted to imply regional uplift in the central and northern Tibetan Plateau during this time and is consistent with the idea that the associated atmospheric $CO_2$ capture led to the Eocene-Oligocene climate transition. However, these findings open new questions to solve: what is the precise relation between Asian aridity and global climate cooling? Is the high vegetation appearance related to uplift only? What is the variability of the climate before the Eocene-Oligocene transition?

To unravel the interplay between regional aridification, global cooling and uplift of the Tibetan Plateau, we present here results of a more detailed, higher resolution palynological study of the key period leading to the Eocene-Oligocene transition as recorded in one of the previously studied sections (the Shuiwan section) from the Xining sub-basin. Moreover, this study produces a reference palynological record of regional aridity in China during the Eocene, including in particular a thorough description of representatives of the xerophytic Nitrariadites group. This group dominated during the Paleogene but strongly diminished during the Neogene. The palynological reference, with an accurate palaeomagnetic age control, includes high quality pictures of typical Eocene Chinese pollen as well as translations of the original taxonomic descriptions that were originally published in Chinese.

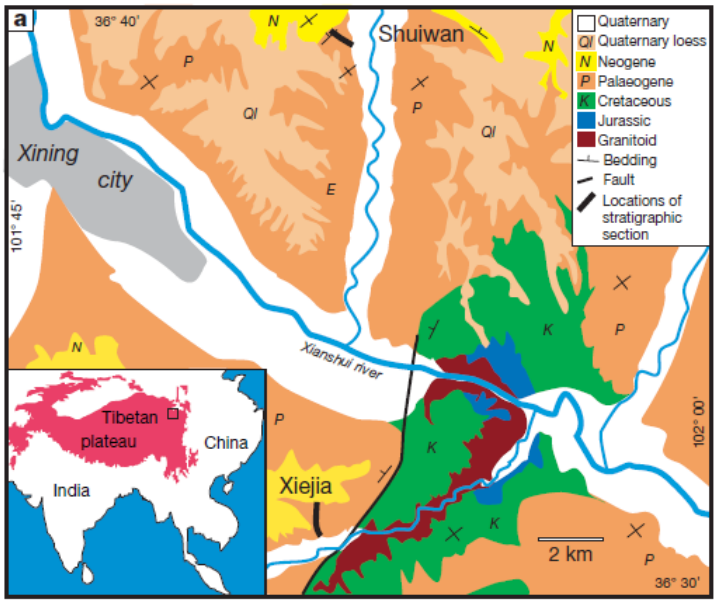


*Figure 1.Locations of the Xining sub-basin and the Shuiwan section (Dupont-Nivet et al., 2008).*

# 2. Geological and palynological background of the Xining sub-basin

## 2.1 Tectonic setting

Tectonic deformation during the late Mesozoic and Cenozoic growth of the Tibetan Plateau resulted in active rift basins in the east of China and compressional depression basins in the west. In total more than 200 sedimentary basins with Cenozoic clastic sediments have been identified, a few of them including non-marine sediments of Paleogene age. The studied Xining Basin is one of these basins. It is located at the northeastern margin of the Tibetan Plateau. It probably began as a fault controlled high subsidence basin during the Late Jurassic-Early Cretaceous, but the part of interest for us relates to subsequent slow subsidence yielding slow accumulation of Paleogene lacustrine sediments (Horton et al., 2004; Sun and Wang, 2005). During the Miocene, subsidence was disrupted by shortening related to the Indo-Asian collision, resulting in localized range uplift and enhanced flexural subsidence and basin compartmentalization. Consequently the Longzhong Basin was divided into sub-basins: the Xining sub-basin to the west, the Lanzhou and Longxi sub-basins to the east and the Linxia sub-basin to the southwest. At present these adjacent basins are situated at 1500-3000 m elevations above sea level (Dai et al., 2006; Horton et al., 2004).

## 2.2 Stratigraphic setting

The onset of deposition in the Xining sub-basin is estimated using magnetostratigraphy at ~55 Ma (Dai et al., 2006). With accurate age control from magnetostratigraphy, the long continuous sedimentary succession in the Xining sub-basin is perfect for studying the tectonic and climatic processes during the Eocene and Oligocene (Dupont-Nivet, et al. 2007).

The Cenozoic successions, in the Xining sub-basin, lie on Cretaceous alluvial sediments or discordantly on older basement rocks. The lower part of this succession consists of sandstones and conglomerates, indicating initiation or reactivation of the basin (references cited in (Dai et al., 2006). This Cenozoic playa to fluvio-lacustrine succession is divided in the Xining and Guide Groups. The Xining Group is subdivided in the QijiaChuan Formation (Palaeocene to possibly lower Eocene), the Honggou Formation (Eocene), and the Mahalagou Formation (Eocene-Oligocene). On top of the Xining Group lies the Guide Group; this is unconformably overlain by the late Miocene to Pliocene Linxia Group (references cited in (Dai et al., 2006)).

The Eocene-Oligocene global cooling characterized by intense aridification in NW China is well recorded in the Xining Group where a sudden change from evaporites to exclusively red clays represent a change from playa-lake environment to distal alluvial fan environments (Dupont-Nivet et al., 2007; Talbot and Allen, 1996). The evaporites hold an excellent palynological record that provides detailed information on the Late Eocene regional vegetation development up to the Eocene-Oligocene transition. This study focuses on the pollen record from these evaporites found in the Eocene to Oligocene Honggou and Mahalagou Formations.

The Honggou Formation consists of red-orange sandstones, and green-white muddy gypsum (Dai et al., 2006; Horton et al., 2004). The gypsum layers in the lower part of the succession are laterally continuous and formed by decimeter- to meter thick tabular, nodular or laminar beds of albastrine massive gypsum. These beds grade into green mudstone with lacustrine laminations (Dupont-Nivet et al., 2007). In the Mahalagou Formation green-white muddy gypsum grades into red gypsiferous

mudstone. The gypsum layers are thought to be formed during wetter periods and the mudstones during dryer periods. The alterations of laterally continuous gypsum layers and red mudstone beds in the lower part of the stratigraphy are interpreted by Dupont-Nivet et al. (2007) and by Dai et al. (2006) as lacustrine saline playa to distal alluvial fan deposits and suggest little local tectonism and slow accumulation during this time (Figure 2). In the upper part of the Paleogene succession gypsum layers disappear. The stratigraphy is dominated by red mudstones with minor gypsum intervals and sandstone layers. This is indicative of a distal alluvial fan depositional environment, without any playa lakes. Regional disappearance of gypsiferous playa lake deposits is dated on the Eocene-Oligocene transition, and indicative of aridification of the environment (Dupont-Nivet et al., 2007).

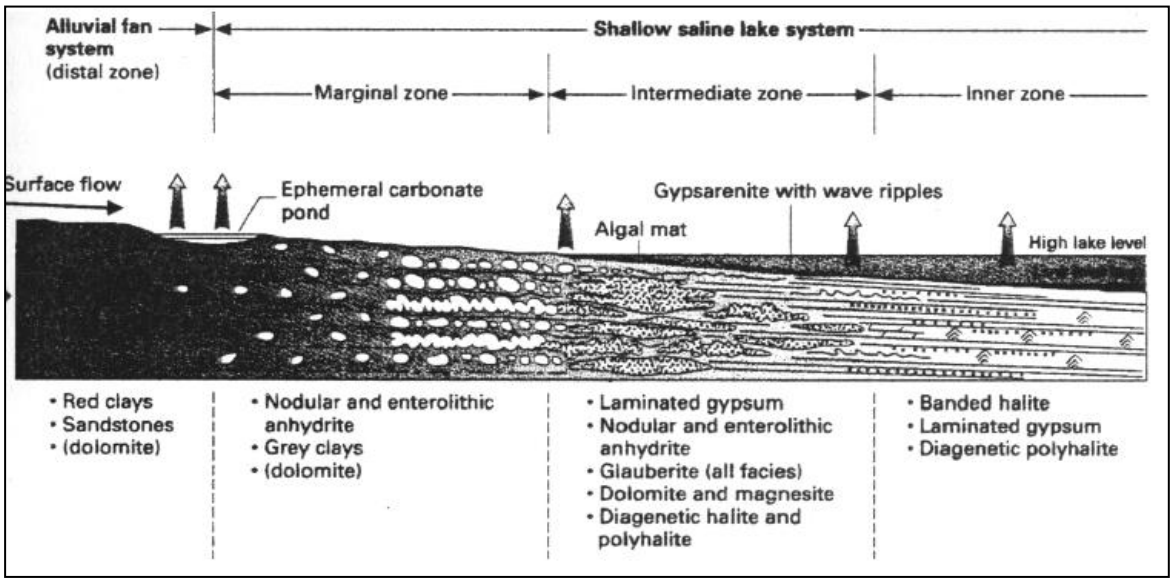


*Figure 2. Depositional environment; saline lake system with distal alluvial fan system (Talbot and Allen, 1996).*

## 2.3 Palynological setting

### *2.3.1 Eocene Palynology*

Different references describe pollen assemblages of China. In this section we synthesized some of these palynological data. The description starts on a regional scale and will zoom in on the Xining sub-basin. Emphasis lies on the Paleogene (Eocene) pollen assemblages, since this is the time-span of interest for this study.

#### *2.3.1.1 China*

Based on Paleogene sporopollen assemblages China was divided in three latitudinal vegetation zones during the Eocene, which can be identified as follows (Sun and Wang, 2005):

Subtropical humid vegetation covered northern and northeastern China during Eocene times. Fossil pollen of this zone denote a mixed broadleaved deciduous and evergreen forest, flourishing under humid subtropical conditions (Sun and Wang, 2005). Assemblages from this humid area are composed of mesophilous and hygrophilous taxa, e.g. *Polypodiaceaesporites, Taxodiaceaepollenites, Cedripites, Quercoidites* and *Cupuliferoipollenites (Li and Zhang, 2000).*

Subtropical to tropical arid to semiarid vegetation was typical for middle China in the Eocene. The Xining sub-basin was situated in this vegetation belt during the Late Eocene. The pollen data suggest desert vegetation mainly from *Ephedripites, Nitrariadites, Euphorbiacidites, Chenopodipollis* and *Labitricolpites.* Especially in the northwest these xerophytic taxa were dominant and were mainly distributed across the basins, trees occurred on the mountains. The climate was probably warm and dry (Li and Zhang, 2000; Miao et al., 2008; Sun and Wang, 2005).

Southern China knew tropical humid conditions during the Eocene. In the early Eocene pollen diversity was very low and the palm (*Monocolpopollenites*) dominated the assemblages, indicating tropical vegetation and a hot, humid climate. Later temperate taxa mixed with tropical and subtropical plants replaced palm and dominated the pollen assemblages. During that time Salicaea, Betulacaea, Fagaceae, Ulmaceae, Juglandaceae, Altingiaceae, Myrtaceae, Lauraceae, Pinaceae, Polypodiaceae and Lygodiaceae were main components of the palynoflora of the southern humid zone. At the same time a large number of fresh water algae (e.g. *Pediastrum*) and a water fern (*Ceratopteris*) occurred. Representative for a warm, humid and mainly terrestrial environment at the middle Eocene (Li and Zhang, 2000; Sun and Wang, 2005). Global cooling and increased tectonic movement, resulting in uplift of mountainous areas, caused Pinaceae plants to increase in all three vegetation zones during the Paleogene. This period of abundant Pinaceae pollen appearance is called the 'Pinaceae pollen phase' (Gao et al., 2000).

#### *2.3.1.2 North west China*

The Xining sub-basin is located in the northwestern part of China. During the Eocene this northwestern part was a component of the subtropical to tropical arid to semiarid vegetation zone. As mentioned before *Ephedripites, Nitrariadites, Euphorbiacidites, Chenopodipollis* and *Labitricolpites* pollen assemblage is thought to be representative for this arid zone. During the Late Eocene gymnosperm and angiosperm pollen was abundant in this area. The gymnosperms consisted of conifers (i.e. *Pinuspollenites, Abietineaepollenites*, *Piceaepollenites*, *Abiespollenites*, *Cedripites* and *Podocarpidites*) and *Ephedripites.* Values of *Nitrariadites* and *Chenopodipollis* were high. Broad leaved forest taxa become abundant (i.e. Betulaceae, *Ulmipollenites*, *Juglanspollenites*, *Engelhardtioidites*, *Pterocaryapollenties, Salixipollenites, Cupuliferoipollenites* and *Quercoidites*). The fern spores were rare, mainly including *Pterisporites.* The palynoflora indicates that subtropical forest, semiarid shrubs with open forest existed in northwest China during the Late Eocene (Miao et al., 2008).

#### *2.3.1.3 Xining sub-basin*

Jurassic-Cretaceous palynological assemblages are dominated by gymnosperms and pteridophytes, with small proportions of angiosperms in Upper Cretaceous strata (Horton et al., 2004). In the late Cretaceous, pollen assemblages are dominated by *Shizaeoisporites* and *Ephedripites*, interpreted as an arid climate (Sun and Wang, 2005).

During the Paleocene the *Shizaeoisporites* decrease significantly, and the pollen assemblages are dominated by *Ephedripites*. Proteaceae pollen values increase and *Nitrariadites* occurs in trace amounts. Also tropical and sub-tropical plants including *Quercus, Castanopsis, Engelharditia, Liquidambar, Nyssa,* Sapindaceae, Rutaceae, *Nanlinpollis* and *Jianhanpollis* occur, reflecting an arid climate with a relatively high average temperature (Sun and Wang, 2005). According to Horton et al.

(2004), and the references cited in this article, the Paleocene to possibly lower Eocene Qijiachuan Formation contains also the palynomorphs *Scabiosapollis* and *Normapollis*.

During the Early Eocene *Ephedripites* decreased significantly and increased sharply again in the middle and late Eocene. Proteaceae pollen almost disappeared, and *Nitraria* increased in the middle and late Eocene (Sun and Wang, 2005). The high percentage of a triporate pollen type, equivalent to modern *Celtis,* and palynomorphs *Quercoidites, Ulmipollenites* and *Iodes* (Horton et al., 2004) probably represents the development of a temperate and humid climate in the Eocene. From the Late Eocene to Early Oligocene *Ephedra* clearly increase obviously, and the climate becomes more arid again (Wang et al., 1990). The Eocene climate seemed thus variable with more humid early stages and drier later stages.

*Ephedra* keep increasing, as well as coniferae in the Oligocene (Wang et al., 1990). Pollen of arid plants dominated the assemblages in the early and middle Oligocene, *Ephedripites* and *Nitraria* occur in large amounts and Chenopodiaceae in small amounts. *Celtis* pollen decreases and pollen of conifers, such as *Pinuspollenites* and *Piceaepollenites*, appears and increases. The climate still appears dry, but cooler (Sun and Wang, 2005). Horton et al. (2004) describes the same palynomorphs in the Oligocene Mahalagou Formation, but also names the palynomorphs *Meliaceoidites* (the palynomorphs of Meliaceae and *Nitraria* are hard to distinct, and fossil pollen grains of *Nitraria* can sometimes be considered as pollen grains of Meliaceae). Dupont-Nivet et al. (2008) dated the appearance of the coniferous types before the Eocene-Oligocene transition and describes a somewhat different pollen assemblage. According to their study the assemblage before the conifer appearance is characterized by *Eleagnacidites, Retitrescolpites* and *Brochotriletus* and different taxa of the *Retitricolpites* group. These taxa decrease and disappear at the appearance of the Pinaceae family. Herbs of the Chenopodiaceae, Amaranthaceae, Caryophyllaceae (CAC group), Poaceae, and Compositae, are nearly absent in the lower part of the formation, but emerge around the conifer appearance and increase toward the Eocene-Oligocene transition (Dupont-Nivet et al., 2008, 2009).

The pollen assemblages of the late Oligocene differ considerably from the assemblages of the early Oligocene. *Ephedripites* and *Nitraria* decrease and Chenopodiaceae increases. Conifer pollen values are higher, including *Piceae, Tsuga, Pinus, Abies* and *Cedrus (Sun and Wang, 2005).*

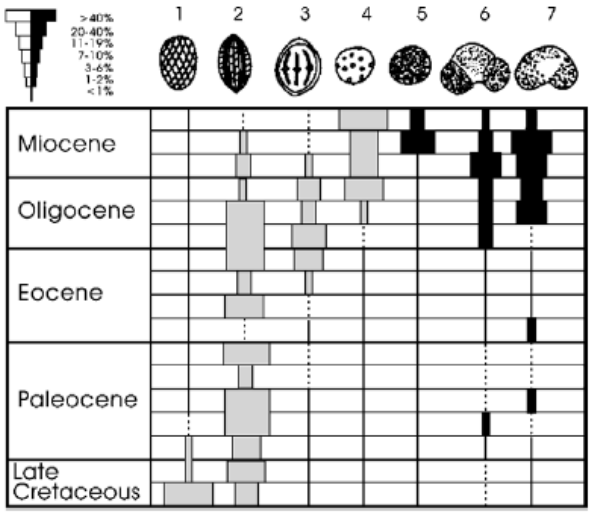


*Figure 3. Diagram of typical pollen types of the Xining sub-basin. Grey bars indicate the xerophytic pollen taxa, black bars indicate more humid pollen taxa. 1. Schizaeoisporites; 2. Ephedripites; 3. Nitrariadites; 4.Chenopodipollis; 5.Potomogeton; 6. Pinuspollenites; 7. Piceaepollenites (Sun and Wang, 2005)(modified from(Wang et al., 1990)).*

### *2.3.2 Modern vegetation*

In general, the modern vegetation in the Xining basin is sparse, and due to the cool and dry environment grassland and shrubs dominate. In this region grasses are primarily composed of Gramineae (*Stipa bungeana and S. breviflora*), Compositae and shrubs (*Reaumuria soongoric, Peganum harmala and Nitraria*)(Liu et al., 2007; Sun and Wang, 2005).

# 3. Methods

Pollen will be the key proxy to investigate the palaeoenvironment and palaeoclimatic conditions of the Xining sub-basin. Yu et al. (2001) proved the good agreement between modern vegetation and modern surface pollen samples across the Tibetan Plateau, which provides a measure of the reliability of using pollen data to reconstruct past vegetation patterns. Specific suites of fossil pollen taxa can be used to reconstruct past vegetation patterns, e.g. steppe, cold evergreen forest, deciduous broadleaved forest, tropical-subtropical forest. Therefore palynological analysis of fossil pollen assemblages is a powerful method for reconstructing palaeoenvironmental conditions (Dupont-Nivet et al., 2008).

## 3.1 Sampling method

In principle, the sampling was aimed at choosing the rocks that have potentially best preserved pollen. The dry playa-lake environments of the sampled Paleogene basins from northeastern Tibet provide ideal conditions for pollen preservation. The outer part of the pollen wall, the exine, is constructed of durable polymers, and its function is to protect the gametophyte. The majority of pollen mainly fails to reach their destination; it is eaten by animals, degraded by microbes or oxidized. Pollen exines may survive only where consumers and decomposers are scarce, such as in anaerobic, saline or very dry environments. Low microbial activity is thus the basis for pollen survival and fossilization (Moore et al., 1991). Pollen grains are well preserved in playa-lake sediments, due to

the low rates of deposition of fine clastics, the wet, spacious and sticky surface, which act as a trap and the good insulation of pollen by periods of drying up, protecting pollen grains against corrosion by oxidation (Horowitz, 1992). Playa-lakes receive water, sediment and inwashed pollen from their drainage system. In addition pollen will arrive from the atmosphere; pollen composition of arid areas depends largely on aerial pollen deposition (Cour et al., 1999). Therefore this environment is a typical site for pollen analysis, giving a regionally integrated vegetation record (Huntley and Webb, 1988). For these reasons playa-lake deposits, represented as gypsum beds, were sampled for pollen analysis.

In the study area, muddy gypsum and green mudstones were chosen to collect samples from, since these have been less oxidized and pollen has been best conserved. In addition, dark, carbon rich mudstones and lacustrine muddy limestone horizons were sampled. Sampled material was selected as fine as mud and not coarser, since the granulometry of pollen is similar to mud such that pollen is deposited together with the mud. It was important to collect fresh samples to reduce the chance of contamination of the samples by modern organic matter. Since most previous samples yielded low pollen concentrations, relatively large samples (~500 grams) were collected. Samples were taken at regular intervals in the stratigraphy. They were collected by carefully extracting fresh pieces of sediment from dug pits with the help of a hammer and a clean knife blade to avoid contamination from present-day pollen or slope deposits. Of each sample location, lithology and depositional environment were described, photographed and carefully positioned in the stratigraphic logs of the sections.

Samples were taken at the following localities: at the Dahonggou section (DHG) near the city of Lanzhou and at different sections around the city of Xining: the East Xining section (EX), the Shuiwan section (SW), the Xiejia section (HGX) and the Tiefo section (TF). At the Ledu section, close to the village Ledu in between Lanzhou and Xining, and at the Pingan section next to Xining only a few more samples were taken and are therefore not further discussed.

In total around 180 samples were collected. The main focus was on the East Xining section to study the Honggou Formation interval. This section has been sampled in high resolution, 80 samples were taken. The other main section was the Shuiwan section; this section was sampled earlier, but this time in higher resolution with 54 samples, to study the younger Mahalagou Formation interval. The Tiefo section consists of the top of the Honggou formation and is the link between the East Xining section and the Shuiwan section; in this section 10 samples were collected. A small part of the Honggou Formation at the Xiejia section has also been sampled, with 15 samples. The Lanzhou area, around 200 kilometers to the east of Xining, has been sampled to study the regional correlation between the two areas; 18 samples were collected at the Dahonggou section in this area. The Ledu section and Pingan section were sampled to see if the sections are interesting for further research.

For this study not enough time was available to process and analyze all the collected samples. The focus of this study is therefore only on the Shuiwan section, since an earlier study on this section offered good results. In addition there is a accurate age control on this section; the ages of the sites were determined by palaeomagnetism.

## 3.2 Preparation of samples

Sediment samples were prepared for pollen analysis by physical and chemical treatments to remove non-pollen matter and to concentrate the pollen grains. The palynological processing was done with help of Ing. M. Konert at the Sediment Laboratory of the Vrije Universiteit, Amsterdam. A specific method was devised to extract pollen from gypsum beds following a modified version of a technique originally proposed by A. Horowitz ('Palynology of Arid Lands', 1992) and described in the data repository of Dupont-Nivet et al. (2008):

1. 50 to 100 grams were selected from each sample and washed to minimize the chance of contamination by modern pollen. The samples were dried and crushed, although complete crushing was avoided, this to keep the pollen intact.

2. The samples were placed in 800 ml containers, submerged in diluted hydrochloric acid (10%), and heated to boiling point to digest the carbonates in the samples. The sediment was topped with demineralised water and left to rest for circa 12 hours.

3. The liquid was decanted, and refilled with water. This process was repeated two times until the suspension became completely transparent and pH neutral.

4. The samples were then submerged in sodium pyrophosphate (1%) and heated to boiling point and then left to cool down. Sodium pyrophosphate is used as a deflocculant in the preparation of clay-rich materials (Moore et al., 1991).

5. The samples were brought in suspension and sieved in small portions over an 8 µ screen. This sieve is so fine that it retained pollen along with coarser materials, and allow finer particles to pass through, this to wash out the finer clay particles. Clay particles had to be removed since they are charged, and can create flakes in the mixing-machine. Also clay particles can obscure the pollen grains.

6. The residue was split over 4 centrifuge tubes (15ml each), followed by heavy liquid separation by sodium polywolframate of density 2.0. As the density of sediment is larger than 2.0 this formed the sink and the pollen and other organic matter floated because of its smaller density. This separation was repeated once and the 4 floating parts were added together resulting in one pollen residue for each sample.

7. The residues were washed several times with demineralised water until the liquid was clear, this to wash out the last clay particles. To remove the very last silica present 10 µl HF was added.

8. Glycerine was added and the residues were dried in the oven.

9. Finally the residues were mounted in 'Kaisers' glycerine-gelatine and sealed with paraffin. The advantage of glycerine-gelatine is that it can be easily handled, being molten at higher temperatures and solid at room temperature. It also has excellent optical properties. A disadvantage is that the glycerine-gelatine absorbs atmospheric water, which causes the pollen grains to swell and increase in size by 1,25-1,5 times (Moore et al., 1991).

## 3.3 Analytical method and reference literature

Slides were examined using a binocular microscope. The basis of pollen analysis is identification and counting of the pollen grains (Moore et al., 1991). Individual pollen grains can be identified to family, genus and species. Identifications are confirmed with the aid of reference collections. First, the most common pollen types had to be learned before counting. For scanning and counting the prepared slides a magnification of x1000, i.e. x100 objective and x10 eyepiece, was most appropriate. Scanning was done by means of linear traverses passing from one edge to the other, this to overcome the pattern that larger grains are more frequent in the centre of the slide and smaller grains at the edges.

A living pollen grain has a wall that is made up of two layers. The outer layer is the exine and is composed of sporopollenin. The inner layer is the intine and made of cellulose. During fossilization only the resistant exine remains. Identification of pollen grains is based on the characteristic form and sculptures of this exine. For identification one of the first features to note are the apertures. Apertures are thin or missing parts in the exine. There are two sorts of aperture, pori and colpi. Colpi are long and boat-shaped with pointed ends. Pori are isodiametric apertures. Pollen grains can be divided in different groups on the basis of the number, position and characters of their apertures. In addition, the shape of a grain can be useful in identification, although the use of size has been avoided as the size can vary between grains of the same species. After classifying the pollen grains in separate groups based on their apertures, these classes can be further divided, considering the fine structure and pattern of the exine (Moore et al., 1991).

For identification of the pollen grains the reference collection of Jansonius et al., Genera File of Fossil Spores, was consulted. Lists of pollen taxa in Wang et al. (1990) and in Zhang and Zhan (1991) were used to select the specific taxa from this reference collection.

Pollen types were morphologically grouped (i.e. triporate, tricolporate, etc.) and classified according to their corresponding vegetation types (i.e. xerophytic vegetation, conifer forest, etc.), mainly following Yu et al. (2000). Affinities were partly traced with help of Song et al. (2004).

## 3.4 Plotting diagrams

To display outcomes of the pollen analysis a pollen diagram is the traditional graphic method. This pollen diagram consists of series of profiles of individual pollen types. The vertical axis represents the stratigraphic level and age of the sediments; the horizontal axis of each profile is the percent concentration of pollen for several pollen types (Huntley and Webb, 1988). In the form of analysis where pollen taxa are expressed as a percentage of the pollen sum, numerical problems can arise. This is because of the influence of each type upon the others, since the pollen sum must always maintain 100%. Never one component of the pollen assemblage is varying, but some types will move in concert, others vary in the opposite direction because of competitive and community interactions. This problem becomes severe if local pollen taxa have a high input and undergo large fluctuations (Moore et al., 1991). To aid interpretation of pollen diagrams, they are often divided into pollen assemblage zones, a biostratigraphic unit, only defined upon its pollen content.

Plotting the diagrams was initially done using C2, which is a Windows program, written by Steve Juggins at Newcastle University. C2 is free to download and use but the data analysis and graphics

functions are restricted to a maximum number of 75 samples. This software is easy to manage and gave a good first impression.

Most diagrams were later computed and plotted using the latest version of Tilia, since this program provided more of the needed options. This program is developed by Dr. Eric Grimm at the Illinois State Museum. Preparation of the data, i.e. pollen sum and percentages calculations, was done using the MS-DOS program Tilia version 5. The prepared data were plotted in the Tilia TGView program. In this program extra features could be added to the diagram, such as groups and zones. CONISS carries out Constrained Incremental Sums of Squares cluster analysis, which was applied and partly used as a basis for zonation. This method works by searching the dataset for the two most similar, stratigraphically-adjacent, samples, and combining them. The combination is then treated as a single sample, and the search is repeated (Grimm, 1987).

The plotted diagrams in Tilia TGView and C2 have been exported to and adapted in the graphics editor Adobe Illustrator.

## 3.5 Photos

### *3.5.1 Differential interference contrast microscopy*

Important fossil pollen grains were documented by microphotography. Nomarski Differential Interference Contrast (DIC) microscopy with a photographic system was used to image these pollen grains at high resolution. Most illustrations were made with a x63 oil immersion objective, and with a x8 photo eyepiece. Very large grains were photographed with a x40 oil immersion objective. The digital technique used is referred as manual z-stacking, indicating the varying z-axis while making the images. The resulting images have been manually combined in Photoshop, since automatic stacking would give complications. Stacking the different layers in depth gives images comparable to 3D images. Appendix 4 contains photos of typical Eocene Chinese pollen grains obtained by this technique.

### *3.5.2 SEM*

Pollen images were generated on the Zeiss DSM 960 Digital Scanning Electron Microscope by R. Zetter of the Department of Palaeontology, University of Vienna, Austria.

The following method, described by Ferguson et al. (2007), was used to produce the pictures. With a pipette a drop of glycerin with pollen was transferred to a glass slide. Using a dissecting needle to which a nasal hair has been affixed, the grains which are of particular interest were brushed out of the glycerin. The pollen was transferred to an aluminum SEM stub to which a drop of absolute ethanol has been added. The ethanol removes all traces of the glycerin from the surface of the pollen grains, so that these can be examined in great detail under the SEM. The stubs were sputtered with gold in a BIORAD Sputter Coater for 4 min before being examined in a SEM at 10 kV.

## 3.6 Comparison with recent vegetation and biome interpretation

It is only possible to say something about the past vegetation and the past environment by using the present as a key to the past. Therefore nearest living relatives were assigned to the fossil plants, where needed with aid of Song et al. (2004).

Finding a present day environment that includes as many of the relatives as possible is the second step. From the characteristics of that environment a likely palaeoclimate of the region is inferred. Though it should be kept in mind that the assignment of nearest living relatives is the easiest and most reliable for the recent geological past, for Miocene and older times, fossil species are extinct and the conditions in which they lived might have been different (Molnar and England, 1990).

This second step can be made by the method of biome reconstruction; the method of biomization has been fully described by Prentice et al. (1996). First, each pollen taxon is assigned to one or more plant functional types (PFT). This first step produces a relation between PFTs and pollen taxa (a PFT x taxon matrix). By knowing which PFTs occur in each biome, a biome x PFT matrix is derived. Both matrices (PFT x taxon and biome x PFT) are combined to yield a biome x taxon matrix, indicating which pollen taxa may occur in each biome. Finally the pollen samples are each assigned to the biome with which they have maximum affinity (Yu et al., 1998). Yu et al. (1998) have tested the applicability of this procedure, originally developed for Europe, to assign modern surface samples from China to biomes. The procedure successfully indicated the major vegetation types of China.

Classifying the pollen types in their corresponding vegetation groups and the interpretation of the biomes was mainly based on the plant functional types and biome reconstruction described by Yu et al. (2000), although the vegetation types applied in this study are more generalized than the biomes used in the article.

# 4. Results

## 4.1 Pollen types

A total of 84 different pollen types were identified. Most of the taxa were identified with aid of Jansonius' Genera File of Fossil Spores. Pollen taxa of xerophytic shrubs are dominant in all samples, typically *Ephedripites* and *Nitrariadites/Nitraripollis*. The arboreal pollen taxa mainly include pollen taxa of broad leaved forest vegetation in the lower part of the section, and pollen taxa of conifer forest vegetation in the upper part of the sequence. In appendix 1 all the pollen types are listed together with their references. This list is morphologically ordered. Appendix 2 shows all the pollen types, with their nearest living relatives, ordered in groups of vegetation types, following Yu et al. (2000). Appendix 4 illustrates images of typical pollen types for the studied area and age.

## 4.2 Nitraria group

No new species were described during this study, and for the descriptions of pollen types we cited references (Appendix 1).

The *Nitraria* group is most dominant throughout the sequence; this domination is typical for the Eocene of China and is not comparable to Neogene - present palynological spectra. Modern pollen assemblages of dry environments are dominated by *Artemisia* and *Chenopodiaceae.* For that reason this group is described in greater detail.

Nowadays there are only eight species of this genus over the whole world, and five species in Asia. Dozens of fossil species of *Nitraria*, i.e. *Nitrariadites/Nitraripollis,* are widely found in China in Cenozoic deposits. It seems that this genus was widely distributed and originated in Palaeocene and

fully flourished during the Eocene and Oligocene (Song, 2000; Xi and Sun, 1987). Translations of Chinese descriptions of these different species of *Nitrariadites/Nitraripollis* are included as appendix 3.

Some fossil pollen grains of *Nitraria* in Lower Tertiary have been considered as pollen grains of Meliaceae and these pollen types are often confused (Dupont-Nivet et al., 2009; Xi and Sun, 1987). Correct identification is important since *Nitraria* is an indicator plant of arid environments, whereas Meliaceae is a tropical taxon. Distinct differences between both taxa can be observed by LM, SEM and TEM examination.

*Pokrovskaja* is a synonym of *Nitraria*, and although this name was used in older descriptions, we use the latter.

Characteristics of the morphology of *Nitraria* pollen grains are (Xi and Zhang, 1991):

1. Medium large size, the polar axis is 34.8-53.9 µm long and the equatorial axis is 22.6-31.3 µm long.
2. Thick exine, about 3-5.2 µm thick, the exine is extra thickened at the poles.
3. Stratification of the exine.
4. Distinct eye shaped pores with splits at both sides.
5. Sexine is reticulate or almost psilate under the light microscope and striate under the scanning electron microscope.

Appendix 4 partly displays images of the *Nitraria* group, showing the whole variety of species found in the samples. Trying to classify and count the different species did not seem viable at that moment and all the different species were put together in one group.

*Nitraria* is a significant component of the modern vegetation in the study area. Therefore we should be sure that the analyzed pollen is fossilized and no contamination by the modern vegetation took place. Samples were carefully collected and thoroughly washed before preparing to reduce the chance of contamination. Since also a considerable part of the samples are barren (otherwise expected to be also contaminated) we believe that the determined *Nitraria* pollen is of Eocene age.

## 4.3 Pollen record

### *4.3.1 Record of all pollen taxa*

Of the total 54 samples analyzed, 31 samples proved to be productive, containing at least 100 pollen grains, with an average around 300 pollen grains each sample. 23 Samples were barren, failing to provide a satisfactory pollen sum. Results from the pollen analysis are shown in the pollen diagram (Figure 4). For a better visualization only pollen taxa that have a frequency of more than 1% in at least three samples are indicated (Herzschuh et al., 2009). Pollen taxa of xerophytic shrubs are dominant in all samples, typically *Ephedripites* and *Nitrariadites/Nitraripollis* (further indicated by their modern equivalents *Ephedra* and *Nitraria,* respectively). The arboreal pollen taxa mainly include pollen taxa of broad leaved forest vegetation in the lower part of the section, and pollen taxa of

conifer forest vegetation in the upper part of the sequence. Based on the abundances of the different taxa, with help of CONISS, six zones are visually distinguished and described, starting from the bottom up. Some zone boundaries are less viable than others because of the amount of samples they are based on, due to the uneven distribution of productive samples throughout the section.

*Zone A (8 samples, 19.4-36 m, 38.75-37.75 Ma)*

The interpretation of this zone is based on a larger amount of samples, due to higher density of sampled gypsum beds in this part of the section, most of the gypsum cycles having been sampled in a quarry with notably fresher rocks. This quarry comprises the part of the section from 23.6 m until 57.5 m, which can be seen in the corrosion line, indicating low percentages of corroded pollen between these levels. This zone is dominated by pollen taxa of xerophytic vegetation, mainly consisting pollen of halophilous taxa *Ephedra* and *Nitraria.* Both taxa are fluctuating between 20% and 80%. Other xerophytic taxa are less common, with amounts not larger than 5%. Hardly any conifer pollen encounters the samples in this zone. Various broad leaved (temperate and warm) trees appear with low percentages, with highest values for *Fraxinoipollenites* and *Quercoidites* (3cp). The tropical *Monosulcites* is not present in this part of the section. Other taxa appear with low percentages (<5%), *Labitricolpites* and *Retitricolpites* (small) are relatively most abundant. Pteridophytes are rare in this part of the sequence.

*Zone B (12 samples, 36-66.4 m, 37.75-36.42 Ma)*

Again the interpretation of this zone is based on a larger amount of productive samples. This zone is characterized by new appearances and higher percentages of broad leaved, tropical and other taxa. *Ephedra* (10-50%) and *Nitraria* (25-85%) are still the dominant groups and oppositely fluctuate. Other xerophytic taxa are less common, although the CAC group reaches up to around 10%. Coniferous pollen are almost absent in this part of the sequence. Various broad leaved taxa are present with low percentages (<10%). Different broad leaved forest pollen firstly appears in this zone, including *Ostryoipollenites*, *Tiliaepollenites*, aff. Rosaceae, *Cupuliferoipollenites* (3cp) *Engelhardthioipollenites*, as well as the tropical *Monosulcites*, and cf. *Abutilonacidites* and echinate (3c) pollen from the remaining taxa group. Most of these taxa only occur in this zone.

*Zone C (5 samples, 66.4-111.2 m, 36.42-35.04 Ma)*

Less productive samples over a larger interval are available for the interpretation of this zone, making the interpretation less reliable. Vegetation changes in this zone are the most dramatic of the section. The lower boundary is defined by the appearances of coniferous pollen and disappearances of a large amount of broad leaved forest, tropical forest and other taxa pollen. Despite the ongoing domination by the halophilous taxa *Ephedra* and *Nitraria* the conifer pollen significantly rises. In this zone *Nitraria* is clearly the most dominant group (45-65%), *Ephedra* is less abundant (10-30%). Other xerophytic vegetation is still not as common. *Scabiosapollis* with long spines disappears in this zone. Coniferous pollen, mainly including *Pinuspollenites* (further indicated by its modern equivalent *Pinus*) and *Piceaepollenites* (further indicated by its modern equivalent *Piceae*), appears quite abruptly and values of *Pinus* reaches up to 20%. At the top values of conifer pollen decrease again. Most of the broad leaved forest pollen disappears in this zone, and the conifers take over. Some broad leaved forest and other taxa continue in this zone, such as *Caryapollenites*, *Triporopollenites*,

*Cupuliferoipollenites*, with colpi as only apertures, *Quercoidites*, with colpi and pores, *Labitricolpites (minor & major)* and *Retitricolpites,* the smaller variant. Besides *Lycopodiumsporites,* pteridophytes are absent in this part of the sequence.

*Zone D (3 samples, 111.2-128.7 m, 35.04-34.56 Ma)*

This zone is defined by peaks in conifer pollen, including *Pinus, Piceae, Abiespollenites* (further indicated by its modern equivalent *Abies)* and *Cedripites*, with values of *Pinus* and *Piceae* up to almost 20%. Towards the top of the zone the values of the conifer pollen decrease again. Also *Ephedra* shows a peak, with highest values around 40% and lowest values around 15%. *Nitraria* shows a large decline, down to percentages of 20%, increasing towards the top again. *Artemisiaepollenites* peaks in this part of the sequence as well. Most broad leaved trees, other taxa and pteridophytes do not or sporadically occur in this interval.

*Zone E (3 samples, 128.7-160 m, 34.56-34.06 Ma)*

The interpretation of this zone is less viable due to the small amount and uneven distribution of productive samples. This zone differs from the previous zone by the disappearance of most broad leaved forest taxa, other taxa and pteridophytes. Conifer pollen is represented by *Pinus* and *Piceae*, the latter generally increases upwards from 5% to 10%. Other coniferous pollen is not present. Also this zone is dominated by xerophytic shrubs *Ephedra* and *Nitraria.* The former increases upwards to 40%, *Nitraria* decreases and increases again, with an average of 50%.

*Zone F (3 samples, 160-165.4 m, 34.06-33.97 Ma)*

This small zone is based on relatively a large high density of productive samples, although all located above the zone boundary and none below, which makes the interpretation of the boundary position less reliable. The interpretation of this zone is based on appearances and increases of conifer and broad leaved trees, in contrary to the previous zone, lacking these taxa. Conifer forest is represented by *Pinus* (15%), *Piceae* (20%), *Podocarpidites*, *Abiespollenites, Tsugapollenites* and *Cedripites*, hence, an increase in diversity of conifer pollen. Some broad leaved (temperate and warm) taxa and other taxa appear again. The group of ferns and mosses includes *Lycopodiumsporites*, *Verrutriletes*, *Crassoretitrilletes nanhaiensis* and *Undulatisporites. Ephedra* and *Nitraria* values drop, while xerophytic *Compositoipollenites* and *Retitricolpites* (aff. *Tamarix*) values rise.

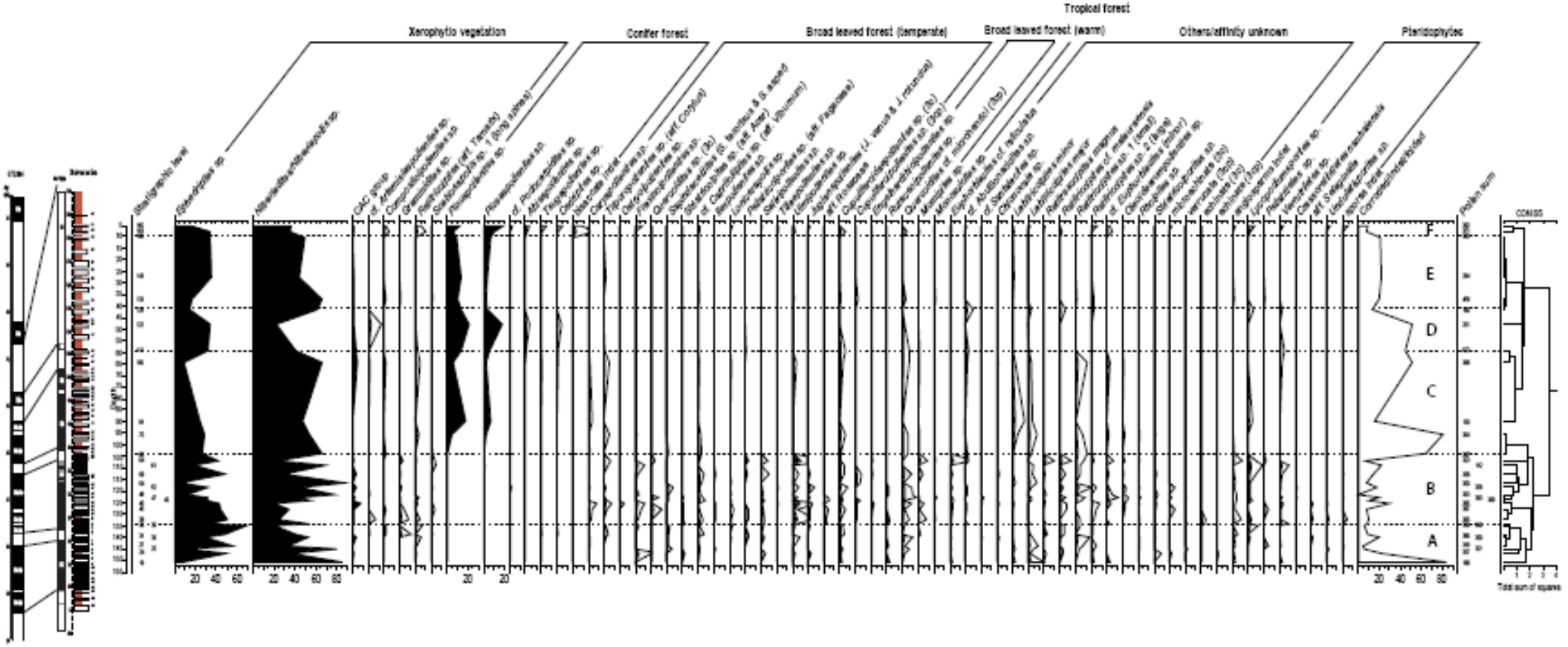


*Figure 4. Pollen diagram of all taxa (magnification by 5 is denoted for the less abundant taxa).*

### *4.3.2 Record of vegetation types*

All the analyzed pollen types are ordered in vegetation types, partly following the biomization of Yu et al. (2000). The groups are indicated at the top of the diagram of all taxa, though for better visualization a separate group diagram is displayed (Figure 5). The diagram is described starting from the bottom up.

Xerophytic vegetation (aff. *Ephedra-Nitraria*) is clearly dominant throughout the whole section, with an average around 80% of the pollen sum. In the lower part of the sequence values of this group significantly fluctuate (between 70% and 90%) due to the higher density of productive samples. The other xerophytic taxa are not as prevailing and do not reach values above 10%. This group shows little increase at the periods of decrease of the *Ephedra-Nitraria* group and vice versa.

Taxa assigned to the conifer forest group are almost absent in the lower part of the section. From stratigraphic level 66.4 m with an age of 36.42 Ma the conifers start to appear and increase in the samples. This group shows three peaks with values around the 40%, and an average of 30%. Where the coniferous pollen is absent in lower zones of the section, broad leaved forest (temperate) taxa are encountered in the samples with average values around 10%. Above the level of appearance of conifers the broad leaved taxa decrease to values not higher than 5% of the pollen sum. Pollen of warm broad leaved trees reaches values up to 5% and shows highest amounts in zone B. Tropical taxa are almost absent with highest values of 3 pollen grains in each sample, only in zone B.

All the remaining taxa, i.e. which could not be classified in the other groups, or from which the affinity is unknown, are put together in one group. This group is mostly present in the lower part of the section, in zones A, B and C. The values fluctuate between 0% and 15%.

The pteridophytes, the sporeplants, including ferns and mosses, fluctuate between values of 0% and 5%, and are also more plentiful in the lower zones, A and B, and in the upper zone F.

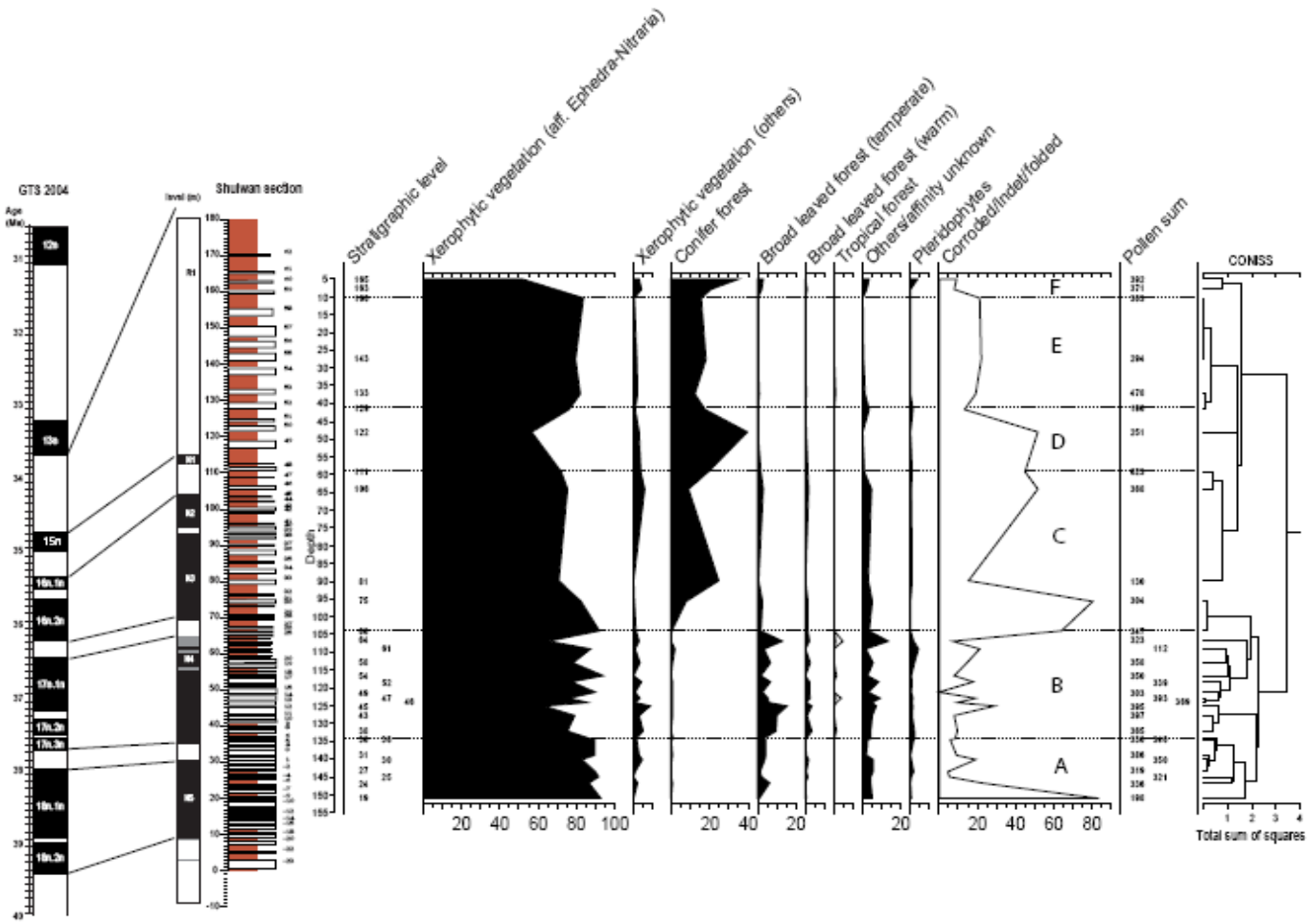


*Figure 5. Pollen diagram of different vegetation types.*

### 4.3.3 Pollen record without local pollen input

In the form of analysis where pollen taxa are expressed as a percentage of the pollen sum, numerical problems can arise. This is because of the influence of each type upon the others, since the pollen sum must always maintain 100%, therefore never one component of the pollen assemblage is varying. This problem becomes severe if local pollen taxa have a high input (Moore et al., 1991). Eliminating the abundant local pollen taxa from the pollen sum and the diagram could partly solve this problem. Figure 6 shows the pollen diagram of the different groups without the local abundant xerophytic vegetation (aff. Ephedra-Nitraria). Some small difference with the previous diagram can be detected, and fluctuations in the different groups are now clearer visible. Although the trends remain more or less the same: broad leaved forest taxa (temperate and warm), other angiosperm taxa and pteridophytes dominate in the lower part of the section, conifers control the pollen assemblage in the upper part of the sequence.

The total regional pollen input or long distance-transport component in the pollen assemblage is indicated by a ratio. This ratio is 100 - xerophytic vegetation (i.e. regional pollen input) over the xerophytic taxa (i.e. local pollen input). Hence, the ratio illustrates the quantity of far transport pollen and the quantity of local vegetation producing pollen relative to each other (Figure 10,B).

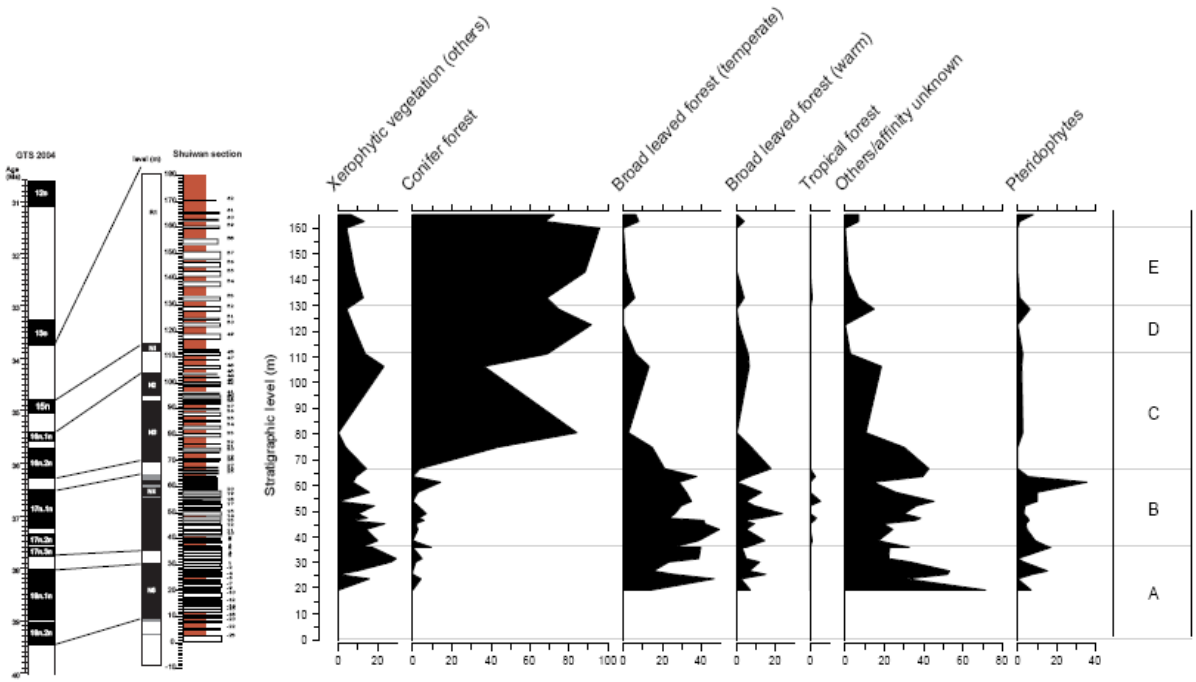


*Figure 6. Pollen diagram of different vegetation types, local abundant pollen of xerophytic vegetation (aff. Ephedra-Nitraria) has been eliminated.*

# 5. Results- Interpretations

In this section the pollen record is interpreted in order to reconstruct the palaeovegetation and the palaeoenvironment of the basin and surrounding regions during the studied time interval. Emphasis lies on the aridity of the palaeobasin, fitting the accepted idea of a subtropical to tropical arid to semiarid vegetation zone covering the central part of China during the Eocene (Sun and Wang, 2005). The second topic of special interest is the Pinaceae appearance, as this is not only a climatic but also a tectonic indicator.

From the pollen data, ratios between taxa can be derived to infer relative aridity of the palaeoenvironment as well as the relative contribution of local versus regional pollen taxa in the pollen assemblage. Both palynology and sedimentology are governed by similar allogenic and autogenic forces, and therefore the relation between the two disciplines is tried to interpret as well.

## 5.1 Biome interpretation

To unravel the past environment and past climatic conditions, different taxa and the climates that characterize their present environments are linked. Nearest living relatives are assigned to the fossil plants, a present day environment that includes as many of these relatives is found (Molnar and England, 1990).

In this study, we follow interpretations of Asian environments based on biome reconstructions by Yu et al. (2000). In an earlier article, Yu et al. (1998) prove that the method of biomization is viable for China and works for fossil pollen as well, although being most reliable for the recent past. In the

tables below, plant functional types and biomes according to Yu et al. (2000) are filtered for pollen taxa found in the here studied sequence. The in this study defined vegetation groups (i.e. xerophytic vegetation, conifer forest, broad leaved forest (temperate/warm), tropical forest, others and pteridophytes) are based on and more general versions of these plant functional types and biomes.

| **Plant functional types** | **Nearest living relatives of pollen taxa found in this study** |
|---|---|
| Arctic/alpine forb/shrub | *Betula, Viburnum* |
| Boreal evergreen conifer | *Pinus, Piceae, Abies* |
| Boreal summergreen | *Alnus, Betula* |
| Cool temperate conifer | *Abies, Tsuga* |
| Desert forb/shrub | *Ephedra, Nitraria, Chenopodiaceae, Caryophyllaceae* |
| Eurythermic conifer | *Pinus* |
| Temperate summergreen | *Acer, Betula, Euphorbiaceae, Quercus* (deciduous), *Rosaceae, Salix, Tilia, Viburnum* |
| Tropical evergreen | Ulmaceae |
| Tropical raingreen | Euphorbiaceae, *Sapotaceae,* Tiliaceae, *Ulmus* |
| Cool-temperate summergreen | *Alnus, Euphorbiaceae, Fraxinus, Lonicera, Ulmus* |
| Intermediate-temperate summergreen | *Alnus, Carya, Cuprifoliaceae, Fagus, Juglans, Lonicera, Ulmus* |
| Warm-temperate conifer | *Cedrus, Podocarpus, Tsuga* |
| Warm-temperate broad leaved evergreen | *Engelhardtia, Quercus* (evergreen) |
| Cool-temperate broad leaved evergreen | *Ilex* |

*Table 1. Indicator pollen taxa and corresponding plant functional types following (Yu et al., 2000), filtered for this study.*

| Biome | Plant functional types |
|---|---|
| Desert | Desert forb/shrub |
| Xerophytic woods/scrub | Eurythermic conifer, Warm-temperate broad leaved evergreen |
| Cool conifer forest | Boreal evergreen conifer, Boreal summergreen, Cool-temperate conifer, Eurythermic conifer |
| Taiga | Boreal evergreen conifer, Boreal summergreen, Boreal evergreen conifer, Eurythermic conifer |
| Cold mixed forest | Boreal evergreen conifer, Boreal summergreen, Cool-temperate conifer, Eurythermic conifer, Temperate summergreen, Cool-temperate summergreen |
| Temperate deciduous forest | Temperate summergreen, cool-temperate summergreen, intermediate-temperate summergreen |
| Broad leaved evergreen/warm mixed forest | Warm-temperate broad leaved evergreen, temperate summergreen, intermediate-temperate summergreen |
| Tropical rain forest/tropical seasonal forest | Tropical raingreen, Tropical evergreen, Warm-temperate conifer, Warm temperate broadleaved evergreen |

*Table 2. Plant functional types and corresponding biomes following (Yu et al., 2000), filtered for this study.*

## 5.2 Local signal

*Ephedra* and *Nitraria* are the dominant groups of pollen taxa throughout the section. Percentages of these groups are high (average 80%) and the associated environment fits not with the environments indicated by the other groups. This leads us to believe that this *Ephedra* and *Nitraria* signal, together with the other xerophytic taxa, corresponds to plants which used to live in the palaeobasin, in the vicinity of the study area during time of deposition

Studies on modern pollen-rain and fossil pollen in China prove that *Ephedra* and *Nitraria* are halophytes, mainly growing in arid environments (Cour et al., 1999; Jiang and Ding, 2008; Li et al., 2009; Ma et al., 2008; Sun and Wang, 2005; Xi and Sun, 1987; Zhao and Herzschuh, 2009). Colman et al. (2007) state that the presences of *Ephedra, Nitraria* and *Chenopodiceae* indicate a treeless alpine desert landscape. As desert plants, their pollen percentages increase with the decrease of precipitation (Herzschuh et al., 2006a; Jiang and Ding, 2008). Desert plant study on the Alashan Plateau, northwest China, shows that plant taxa belonging to Chenopodiaceae, *Nitraria* and *Ephedra* grow mainly on alluvial gravelly plains (Herzschuh et al., 2006a; Herzschuh et al., 2003). Modern

deserts in China cover the most arid regions in the northwest, in most of these regions annual rainfall is less than 100 mm (Sun and Wang, 2005).

The high amounts of *Nitraria* and *Ephedra* indicate an arid to extreme arid environment in the palaeobasin. Values of both pollen types fluctuate through the sequence; these fluctuations seem anti-correlated. Pollen taxa are expressed as percentages of the pollen sum, so each pollen type influences the other types, especially if present in high amounts. However, these relative opposite variations can also be due to competitive interactions. Pollen percentage ratios of *Nitraria* and *Ephedra* (N/E) can indicate the aridity of the environment. According to Li et al. (2005) N/E ratios are less than 1 in typical desert communities, and these ratios are more than 1 in a steppe-desert environment. In figure 7 this ratio of *Nitraria* over *Ephedra* is plotted. The reference line of 1 is indicated in red. When the plotted line is below 1 the environment used to be a typical desert; if the line lies above 1 the environment used to be a steppe desert. The periods of typical desert are colored yellow.

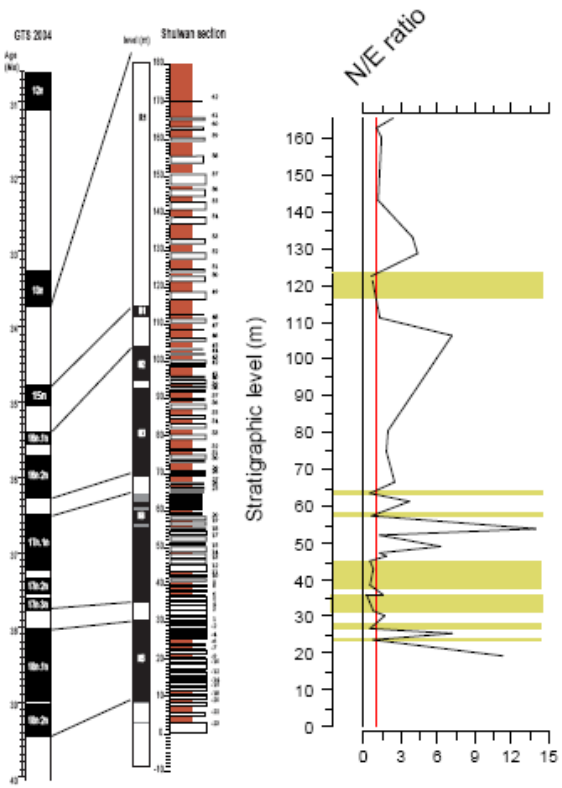


*Figure 7. N/E ratio indicates the aridity of the environment in the palaeobasin. N/E ratio is less than 1 in a typical desert and more than 1 in a steppe desert (red line is the reference line 1). The periods of typical desert are indicated in yellow.*

The pollen data of this study, suggesting arid conditions mainly from *Ephedra* and *Nitraria*, fits in the larger regional picture of China during the Eocene. During this period three latitudinal climatic zones covered China: in the north and south humid conditions prevailed and in middle China semi-arid to arid conditions existed. The Xining sub-basin is located in this subtropical to tropical arid to semi arid vegetation zone of middle China. This broad belt of aridity stretched across China from west to east during the Paleogene (Figure 8) (Sun and Wang, 2005). According to Miao et al. (2008) such wide zonal distribution of semiarid sub-tropical palaeoenvironment is comparable to the Sahara or Australia today.

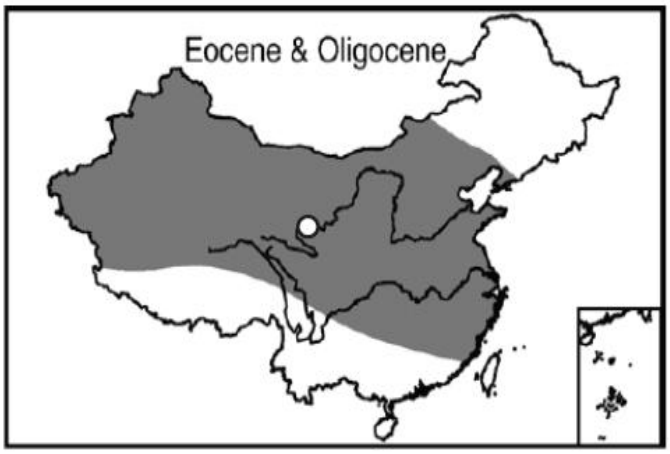


*Figure 8. Palaeoclimatic zones in China during the Eocene and Oligocene. Shaded area is the semi-arid/arid region; circle indicates the location of the Xining sub-basin (Zhang et al., 2007).*

In conclusion, during the whole studied time interval the environment in the palaeobasin was arid, however, extreme arid and relatively more humid conditions alternated. The N/E ratios were likely affected by moisture levels. Unfortunately it is hard to say something valid on the rhythm of the fluctuations, due to the uneven distribution of productive samples through the section. However the density of productive samples is high in the lowest part of the section from 20 to 70 m. In this part of the sequence changes in the variability can be observed. A period of large fluctuations is followed by a period of low variation (25-45 m), which is again followed by a period of higher oscillations. The possible forcing mechanism for these fluctuations will be handled in chapter 6.

## 5.3 Distal signal

Pollen of the broad leaved forest, tropical forest, pteridophytes and other taxa is present in small amounts, and is believed to represent long-distance transport. Arboreal pollen grains can be transported over far distances by air and are found in large-basin lake sediments in treeless arid environments such as that of the past Xining sub-basin. In pollen spectra from such lakes, this far-transport component is generally small when the local pollen production is high, but it is larger when the local vegetation is sparse and its pollen production is low (Cour et al., 1999; Herzschuh et al., 2006b). Hence, the long distance pollen taxa percentages are related to the transport capacity, the production of the long distance pollen taxa, and the local cover density (Cour et al., 1999). The Bisaccate conifer pollen are favored by transport, compared to non-disaccate pollen grains (Fauquette et al., 2006), this explains the relative high percentages of conifer pollen. Hence, whereas the main signal of the dry taxa is thought to be from the palaeobasin itself, pollen of the other

vegetation types is believed to be transported from the periphery, distal from the location of sampling. Cour et al. (1999) proved that some arboreal pollen taxa may be transported over more than 1000 km, and because of its large size, the palaeolake has a large pollen source area, probably comprising 10.000 $km^2$ or more (Jacobson, 1988).

If the main signal of the dry taxa is ignored, one can see that in the lower part of the section (at time interval 38.75-36.42 Ma) the broad leaved forest taxa are dominant. Most broad leaved forest taxa occur from 37.75 to 36.42 Ma. Pollen of the broad leaved forest is present in small amounts and therefore, is believed to represent long-distance transport. Hence, during the time interval of deposition of the lower part of the section broad leaved forest and some other taxa dominated the periphery. The tree pollen indicates the existence of more humid places in the hinterland. Some of the deciduous forest elements are indicative of warm and temperate climates (e.g. *Quercoidites, Caryapollenites, Ulmipollenites, Euphorbiacites*, *Rutaceoipollis*, *Rhoipites*, *Cupuliferoipollenites, Juglanspollenites, Tiliaepollenites, Betulaceoipollenites, Salixpollenites*) (Fauquette et al., 2006; Miao et al., 2008; Sun and Wang, 2005). Also the presence of the subtropical pollen taxa *Engelhardthioipollenites, Sapindaceidites* and *Rutaceoipollenites* reflects a climate with relative high average temperature (Sun and Wang, 2005). In modern equivalent warm-temperate broadleaved deciduous forests in China the annual mean temperature is 9 to 14 ˚C. The annual precipitation is 500 to 900 mm (Sun and Wang, 2005).

From 36.42 Ma, between samples PSW-19 and PSW-18 conifer taxa start significantly to increase. Although conifer pollen is present in higher percentages (average 20%) than other tree pollen, it is thought to be a far-transport component as well. For example *Pinus* pollen may still occur with values in the order of 10–50% in deserts and steppe-deserts, where pine trees are absent, as the result of long-distance transport by wind (Ma et al., 2008). However, percentages of conifer pollen can reach up to 40%, which suggests that the transport distance is not too long (Dupont-Nivet et al., 2008). *Pinus* and *Piceae,* which are the main conifer taxa in this section, are indicative for cool and moist conditions. In a present cold-temperate conifer forest, consisting mainly of *Abies, Piceae* and *Pinus*, the annual average temperature is 2.2 to 5.5 ˚C, and the annual precipitation is 350 to 550 mm (Sun and Wang, 2005). The appearance and presence of conifer pollen after 36.42 Ma, means that somewhere in the periphery a cold-temperate conifer forest developed, indicating cold moist conditions.

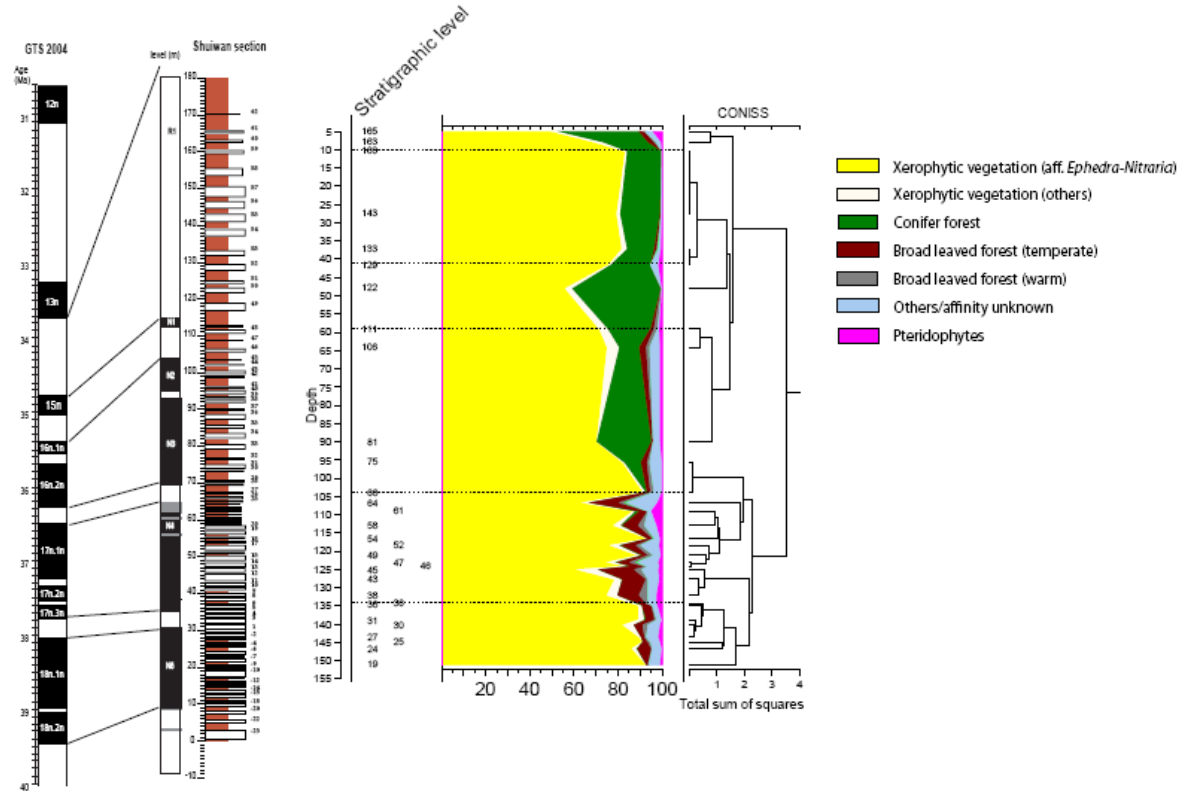


*Figure 9. Stacked diagram of vegetation types.*

Figure 9 clearly shows the presence of broad leaved forest taxa, followed by the appearance of conifer forest taxa, which is typical of different vegetation belts on mountain slopes. High altitude climatic conditions are also indicated by the presence of *Abiespollenites* and *Piceaepollenites,* which present-day analogues optimally occur at elevations from 2500 to 4000 m a.s.l. (Dupont-Nivet et al., 2008; Lu et al., 2008). *Tsugapollenites* and *Cedripites* are high altitude elements as well (Fauquette et al., 2006).The appearance and increase of conifers at 36.42 Ma upwards could be evidence of mountainous areas in the hinterland and, hence, tectonic uplift. It should always be kept in mind that high percentages of pollen taxa, e.g. *Pinus* and *Piceae*, could be due to rework from older sediments. Although in this case this is highly unlikely, because if Pinaceae pollen were reworked from older sediments then we would also expect high values for pteridophytes, being significantly more abundant in earlier times.

Appearance and increase of Pinaceae pollen during the Palaeogene is observed in whole China and this appearance is referred as the 'Pinaceae pollen phase'. It is thought that global cooling and increased tectonic movement, resulting in uplift, are causing this special pollen phase (Gao et al., 2000).

The low concentrations of tropical taxa in the samples indicate that no tropical forest existed close to the palaeobasin. The few tropical pollen grains found, are probably transported over a long distance.

Pteridophytes, indicators of more humid conditions, show low values and therefore believed to be far-transport components as well.

## 5.4 Local pollen input vs. distal pollen input

The far-transport component depends on three factors: the production of the long distance pollen taxa, the transport capacity, and the local vegetation cover. In figure 10 the ratio of the far-transport component ((100-xerophytic taxa)/xerophytic taxa) is compared with the N/E ratio. The latter indicates that either the palaeoenvironment was steppe like or a typical dessert in the basin. We assume that the local vegetation was sparser during the desert conditions. Plotting the two ratios in one graph, a negative correlation between both ratios is indicated by a correlation coefficient .This negative correlation has a significance of almost 50% in the lower part of the section, before the conifers become abundant. Above this level the correlation is less significant. This observation proves that especially lower in the sequence the cover of local vegetation highly influences the percentages of far-transport pollen taxa input. Higher up in the section the effect of the other factors (i.e. long distance pollen production and transport capacity) become more important.

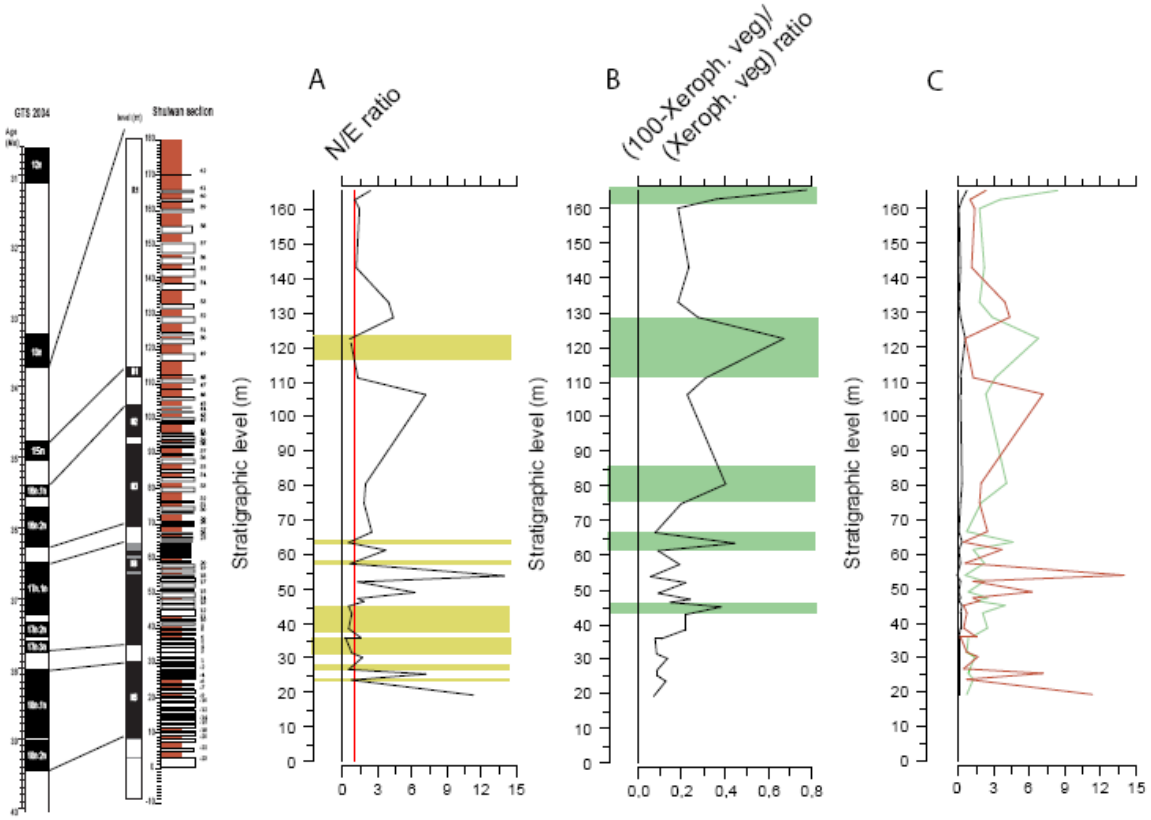


*Figure 10. A) N/E ratio indicates the aridity of the environment in the palaeobasin. N/E ratio is less than 1 in a typical desert and more than 1 in a steppe desert (red line is the reference line 1). The periods of typical desert are indicated in yellow. B) The ratio of non-dry taxa over dry taxa illustrates the regional pollen input relative to the local pollen input. Periods of relatively large regional pollen input is indicated by green. C) Both ratios are compared in the last graph; red is the N/E ratio and green is the pollen input ratio (exaggerated 10 times).*

## 5.5 Correlation palynology and grain size

The study of grain size is beyond the scope of this study, and grain size data were obtained from the MSc thesis by M. Lebbink (2010). The M ratio is the ratio of the fractions 22-44 and 11-22 µm, which is derived from the U ratio by Nugteren et al. (2004). This M ratio is an indicator of the coarseness of the deposited grains.

The M ratio together with the ratio of the regional pollen input over the local pollen input has been plotted in one graph (Figure 11,A). There is a significant positive correlation between the two ratios. This relation is mainly significant (~70%) in the lower part of the section. This positive correlation means that when the grain size increased, the regional input of pollen relatively increased as well, and vice versa, when the grain size decreased, the regional pollen contribution relatively decreased.

Changes of the regional pollen input are relative to the local pollen input; therefore these changes are dependent on the regional pollen input itself and of the local vegetation producing pollen. To explain the correlation between the M ratio and pollen input ratio, two hypotheses are formulated.

The first hypothesis is that the coarseness of the deposited grains depends on the transport capacity, which is associated to the environmental energy flux. A larger environmental energy flux can transport larger grain sizes over larger distances. Also if the transport is higher energetic, more pollen from the periphery can be transported towards the sample location. Therefore it is logical that grain size and the signal of regional pollen input behave similarly, since they are both dependant of the transport capacity.

It is remarkable that the grain size clearly increased from the moment the conifers appeared. So it could be that the appearance and increase of the conifers might have been partly dependant of the increase of environmental energy flux. This would mean that the input of conifer pollen is influenced by some sort of climatic forcing. From the level that the conifers are abundant the correlation between the M ratio and the regional pollen input over the local pollen input is less significant. Bisaccate conifer pollen are favored by transport, compared to non-disaccate pollen grains (Fauquette et al., 2006). Therefore the conifer pollen, mainly present in the higher part of the section, could be transported into the basin, regardless of small energy flux changes. Whereas similar energy flux changes may have had more significant effect on the transport of pollen of the broad leaved forest taxa, lower in the section.

In summary, the first hypothesis supposes that the pollen input ratio highly depends on the regional pollen input, which is associated to the transport capacity, just like the grain size.

The second hypothesis assumes that the pollen input ratio is most dependent on the local vegetation producing pollen. As stated before, the far-transport component can be generally small when the local pollen production is high, and is greater when the local vegetation is sparse and its pollen production is low. This hypothesis supposes that the source of the coarser grains is located relatively closer to the basin; coarser material can only be transported over small distances. If the signal of the regional pollen input is relatively stronger this could mean that the local vegetation is sparser. Sparse

local vegetation can hold less sediments and the transport capacity increases with the decrease of local vegetation.

This last hypothesis fits better with the outcomes of the comparison of the M ratio with the N/E ratio. N/E ratio indicates the aridity of the local environment. When the values of the N/E ratio are relatively low (<1), the environment is extreme dry and a typical desert; when the values are relatively high (>1), the conditions are relatively more humid and the environment is a steppe desert. Vegetation was sparser at levels were the N/E ratio was lowest, because during these times typical deserts existed. In the lower part of the section the M ratio and the N/E ratio are anti correlated, with a significance of ~50%. Lower values of the N/E ratio thus coincide with the higher values of the grain size, and vice versa. During desert conditions, protective vegetation lacks and the ground is dry, making transport of coarser sediments easier. Relative denser local vegetation coverage, during steppe conditions, holds more sediments and less transport of coarser sediments occur. *Nitraria* is an important sand controller and among the soil fixative species that nowadays is used as fodder in dry lands (Boughalleb et al., 2009).

The significance of the correlation between both ratios considerably decreases from the level the conifers appear. The contribution of this long distance transport component is significantly larger than the far-transport component lower in the section. This larger input of regional pollen could have partly overruled the local signal, and therefore the correlation is not as significant anymore.

In summary, the second hypothesis mainly depends on the local vegetation cover. During desert conditions local vegetation is sparser, regional pollen input is larger and coarser material is transported towards the basin. During steppe conditions local vegetation cover is denser, regional pollen input is smaller and coarse sediments are obstructed by vegetation, withholding it to reach the location of sampling.

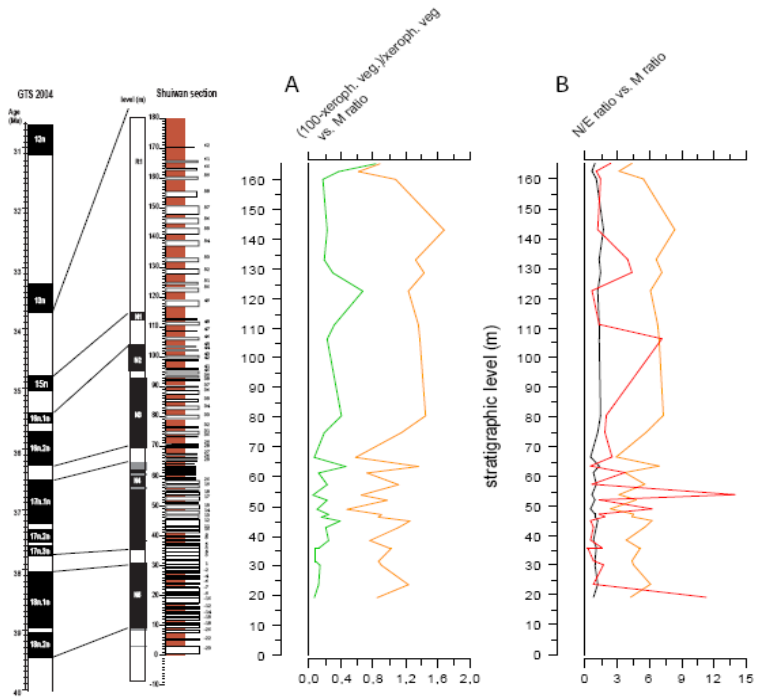


*Figure 11. A) Grain size M ratio (orange) compared to the pollen input ratio (green). B) Grain size M ratio compared to N/E ratio (red). M ratio is magnified by 5 for better visualization (orange).*

# 6. Tectonic uplift vs. climatic control

The key results of this study are in twofold. 1) The main signal of the local xerophytic pollen taxa, with its fluctuations between *Nitraria* and *Ephedra* dominance. 2) The far-transport component represented by the broad leaf forest (warm and temperate) taxa and remaining angiosperms in the lower part of the section, while the conifers characterize the upper part of the section.

Based on the pollen record, the past vegetation has been reconstructed. Vegetation responds strongly to climate. Precipitation and temperature primarily determine the vegetation types, such as forests and deserts (Ruddiman, 2001). The reconstruction of past climate happens in two stages (Horowitz, 1992): the first stage involves defining the characteristics of the palaeoclimate, such as being humid, arid, cold or warm; the second is trying to reason out what may have been responsible for this palaeoclimate, e.g. global climate changes, atmospheric $CO_2$ level, changing sea level and/or tectonics. Hence, the landscape and structural changes, such as uplift, faulting and rift formation may also have an important effect on the palaeovegetation (Horowitz, 1992). So now the question remains what has controlled the palaeoclimate and thus the palaeovegetation in the Xining sub-basin and surroundings during the Late Eocene, in order to try to answer this question below a synopsis of hypotheses is formed.

## 6.1 Local signal

The local pollen input indicates an arid environment during the whole studied time interval, however periods of desert and steppe environments alternate. The fluctuations between extreme arid and

arid conditions depended on the amount of effective precipitation. According to Ruddiman (2001), vegetation changes closely correlate with changes in $\delta^{18}O$ (ice volume). Miao et al. (2008) studied the Eocene palynoflora of the Juiquan Basin, more to the north of the Tibetan Plateau. They suggest that the driest periods coincide with global cooling events. These cooling events are clearly visible in $\delta^{18}O$ records from drilling sites in the tropical Pacific Ocean and near the Antarctic Ocean. Before the Eocene-Oligocene transition long and short cooling was thought to be controlled by several temporary ice caps in the Antarctic (Eldrett et al., 2009; Miao et al., 2008; Tripati et al., 2005) and in the Northern Hemisphere (Eldrett et al., 2009; Tripati et al., 2005). Eocene glacial sediments document mountain glaciations and glaciations in East Antarctica (Ehrmann, 1998). The occurrence of ice-rafted dropstones in middle Eocene sediments from Lomonosov ridge supports early glacial onset in the Arctic (Tripati et al., 2005). Build up of these ice caps, lowered the sea level, decreased oceanic evaporation, and less atmospheric water vapor was available for precipitation. The cooling events around 37 Ma and 35 Ma (Miao et al., 2008) roughly coincide with the most arid periods in our sequence, and the periods of lower $\delta^{18}O$ values generally match the relative more humid phases (Figure 12,b). More could be said about this possible causal link between ice volume and humidity of the palaeobasin if pollen data with higher resolution and over a longer time span was available.

In the lower part of the section (38.75 - 36.5 Ma) enough productive samples are at hand to study the variability of the N/E ratio (Figure 12,b). From 38.75 to 38.25 Ma the variability of this ratio is high; from 38.25 to 37.25 Ma the amplitude is low, and from 37.25 Ma fluctuations are large again. High variability seems to coincide with relative more humid periods, and low variability with extreme arid periods. This could be explained by the fact that transitional vegetation types, such as shrubland (steppe) have higher sensitivity to climatic changes compared to vegetation under extreme climatic conditions, such as deserts (Li et al., 2006). The changes in amplitude of the fluctuations could also reflect the modulations of the eccentricity cycles. To illustrate this, the eccentricity is plotted next to the N/E ratio (Figure 12,a).

Besides air temperature and precipitation atmospheric $CO_2$ is a primary climatic driver. Enriched $CO_2$ levels in the atmosphere greatly enhance growth and water use efficiency in almost all vegetation.
Arid and semi-arid systems are suggested to be among the most responsive to changes in atmospheric $CO_2$ (Smith et al., 2000). Productivity of arid land plants is predicted to increase substantially with rising atmospheric carbon dioxide concentrations due to enhancement in plant water-use efficiency (Housman et al., 2006). Figure 13 shows the atmospheric $CO_2$ levels during the Eocene- Oligocene transition. This transition is not only known for its significant drop in temperature but also for its abrupt atmospheric $CO_2$ decline. Since the signal of the xerophytic vegetation slightly fluctuate around the 80% throughout the whole section it is hard to say anything about the relationship between the atmospheric $CO_2$ levels and the arid plants signal, not a clear correlation can be distinguished.

It is unlikely that local tectonics affected the dry vegetation; we would then expect a transition from one pollen assemblage to another, and no abrupt fluctuations as is observed now. The very low accumulation rates of sediments in the palaeobasin confirms that no major tectonic event has affected the Xining sub-basin during the studied time interval (Dai et al., 2006).

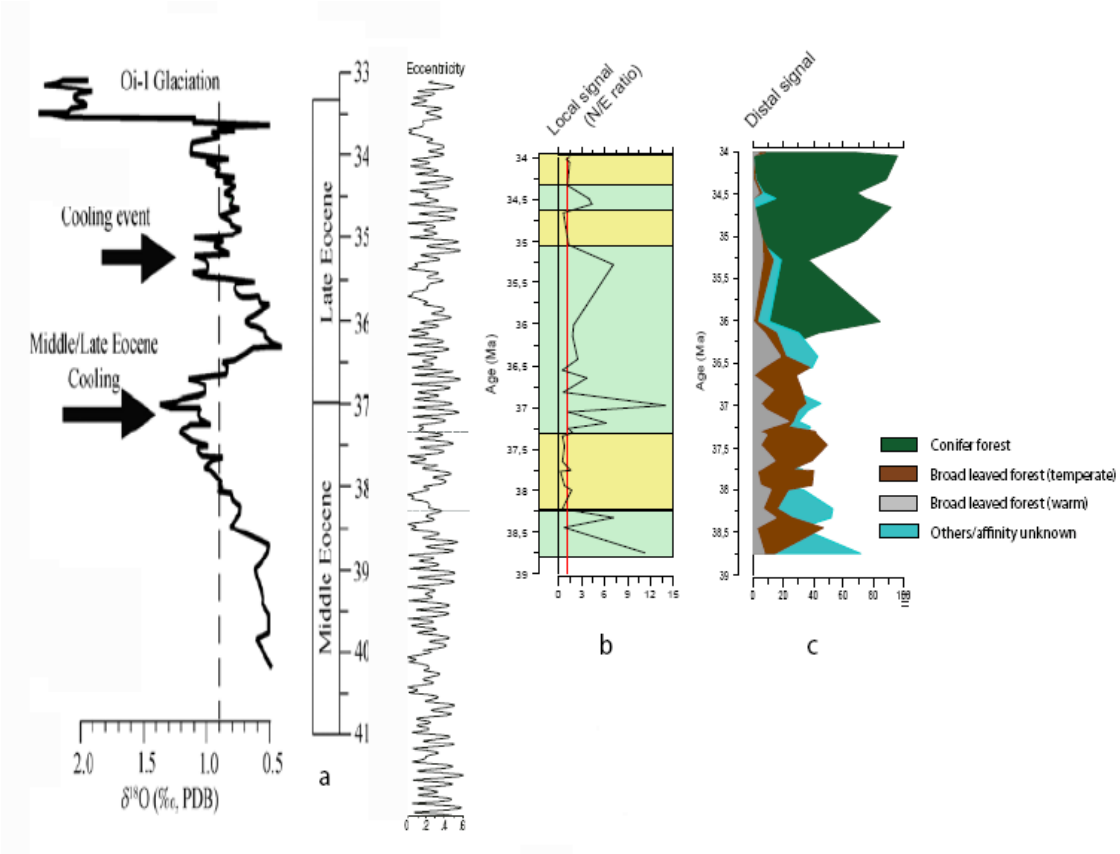


*Figure 12. N/E ratio (b) and distal pollen component (c) compared to stable isotope marine record (Miao et al., 2008; Tripati et al., 2005) and eccentricity line (Dupont-Nivet et al., 2008). In N/E ratio graph extreme arid periods are indicated by yellow and relatively more humid periods are green.*

## 6.2 Distal signal

Palaeoclimate of the source regions of the long distance component do not necessarily have connection with the analyzed site (Horowitz, 1992). Therefore it is reasonable that the local vegetation behavior and distal vegetation behavior do not have to be significantly related.

The results of the long-distance signal show the presence of a broad leaved forest, followed by the appearance of a conifer forest, which is typical of different vegetation belts on mountain slopes. Also the presence of *Abiespollenites, Piceaepollenites, Tsugapollenites* and *Cedripites* are indicating high altitude climatic conditions (Dupont-Nivet et al., 2008; Fauquette et al., 2006; Lu et al., 2008). The appearance and increase of conifers at 36.42 Ma upwards could therefore be evidence of mountainous areas in the hinterland and, hence, tectonic uplift.

Structural and tectonic data supports early uplift of the Tibetan Plateau during the Eocene (Royden et al., 2008; Tapponnier et al., 2001; Wang et al., 2008a; Yin and Harrison, 2000). During the Early Cenozoic the crust was shortened in western and central Tibet and in Eocene-Oligocene times the southern and central part of the Tibetan Plateau were uplifted to high elevations (Royden et al., 2008). Wang et al. (2008a) also hypothesize that central Tibet was uplifted at Paleogene times. Tapponnier et al. (2001) suggest that the growth of the plateau occurred stepwise. The Plateau rose in three steps from south to north. $^{40}Ar/^{39}Ar$ and zircon U–Pb dating of lavas of the central-western

Qiangtang Block proves that the elevation of the central Tibetan Plateau indeed began in Paleogene times, as early as 45–38 Ma ago (Wang et al., 2008b). Also oxygen-isotope-based estimates of palaeoaltitude from late Eocene–Oligocene formations in the Lunpola Basin in central Tibet indicate that the central Tibetan Plateau has been characterized by elevations in excess of 4 km since 35 ± 5Myr ago (Rowley and Currie, 2006). This might suggest that the source of the high altitude pollen was located in Central Tibet, south-west from the Xining sub-basin and transported by the Westerlies.

The tectonic source would have to be distal from the Xining sub-basin since very low sediment accumulation rates governed in the basin itself (Dai et al., 2006). This coincides with the hypothesis that the conifer pollen, originative from the uplifted areas, had been transported over a long distance.

If the regional vegetation, and in special the conifers, was only controlled by global climate changes we would expect the conifer pollen signal more to follow the $\delta^{18}O$ record, and thus appear in the lower part of the section as well. Above the conifer appearance it seems that peaks in the conifer pollen record correspond to lower values of $\delta^{18}O$, and thus to wetter conditions (Figure 12,ab). Also the implication that the grain size considerably increased coeval with the conifer appearance seems that both are influenced by transport capacity and thus are climatically forced.

This gives the impression that the conifer appearance has been mainly controlled by tectonics, but partly by the global climate as well. Eldrett et al. (2009) studied northern high-latitude pollen and spore assemblages for the Eocene and Oligocene interval. Their data indicate a loss or reductions of warm and temperate broad leaved forest taxa and a rise of conifer forest taxa at the end of the Eocene, similar to our results. They lay their findings to ice buildup in the Northern Hemisphere. Also Gao et al. (2000) state that the increase of Pinaceae plants throughout China during the Late Eocene was caused by global cooling and increased tectonic movement. In conclusion, the conifer appearance seems a result of the interplay between tectonics and global climate.

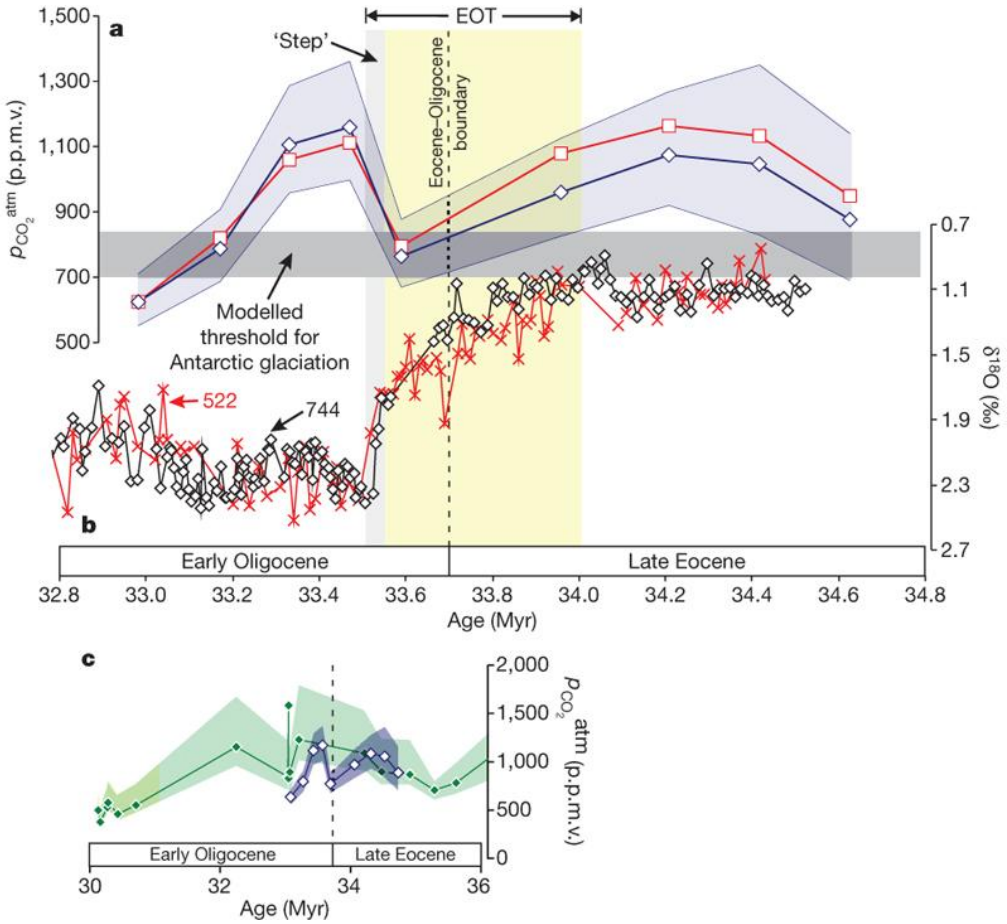


*Figure 13. Reconstructed atmospheric $CO_2$ levels around the EOT (Pearson et al., 2009).*

Rise in atmospheric CO2 concentration directly improves carbon balance and stimulates growth in many tree species. Trees at high altitudes might be particularly sensitive to $CO_2$ enrichment, because they live in an atmosphere of lower partial pressure of $CO_2$ (Hattenschwiler et al., 2002). The current literature indicates a significantly larger average long-term biomass increment under elevated carbon dioxide for conifers than for deciduous trees in studies not involving stress components (Saxe et al., 1998). Again it is hard to differentiate a relationship between the distal tree signal of our study and the atmospheric $CO_2$ levels during the Late Eocene, when plotted together not a clear correlation can be distinguished between the two. To study the connection between atmospheric CO2 levels and enhancement of vegetation growth data over a longer period and in greater detail should be available.

## 6.3 Local signal vs. distal signal

Paragraph 5.4 describes briefly the correlation between the aridity in the palaeobasin and the pollen input from the periphery. This correlation is a negative correlation, that is the long distance pollen input was higher when the basin was dryer, and the distal pollen flux was less when the climate in the basin was relative more humid. Figure 14 shows clearer the opposite phase relationship between the humidity of the basin and the distal signal, hence, indirectly the humidity of the surroundings. Zhao et al. (2010) describe a same sort of pattern in Late Holocene data from the Qaidam Basin. Wet-dry climate shifts show a contrasting pattern at their study lakes in the basin from pollen records in the surrounding mountains, with a dry climate in the basin corresponding with a wet interval in the mountains. They suggest that local topography might have played an important role in mediating regional climate changes, as induced by uplifting air in the surrounding mountains and subsidence of air masses in the basin. Therefore also this contrasting pattern implies that topography, and thus tectonics might have played a role in the vicinity of the study area. However, it is suggested that this opposite phase pattern could only exist when monsoons were very strong. The middle-late Eocene and Oligocene climate in China, was a transitional stage between the planetary wind system of the Cretaceous and the monsoon system developing in the Miocene, and was characterized by variable, weak summer monsoons that brought moisture to the otherwise dry areas (Prell et al., 1998). The opposite correlation between the periphery input and the local input could also be explained by a more direct relationship, since the distal pollen input depends on the local vegetation cover (paragraph 5.4).

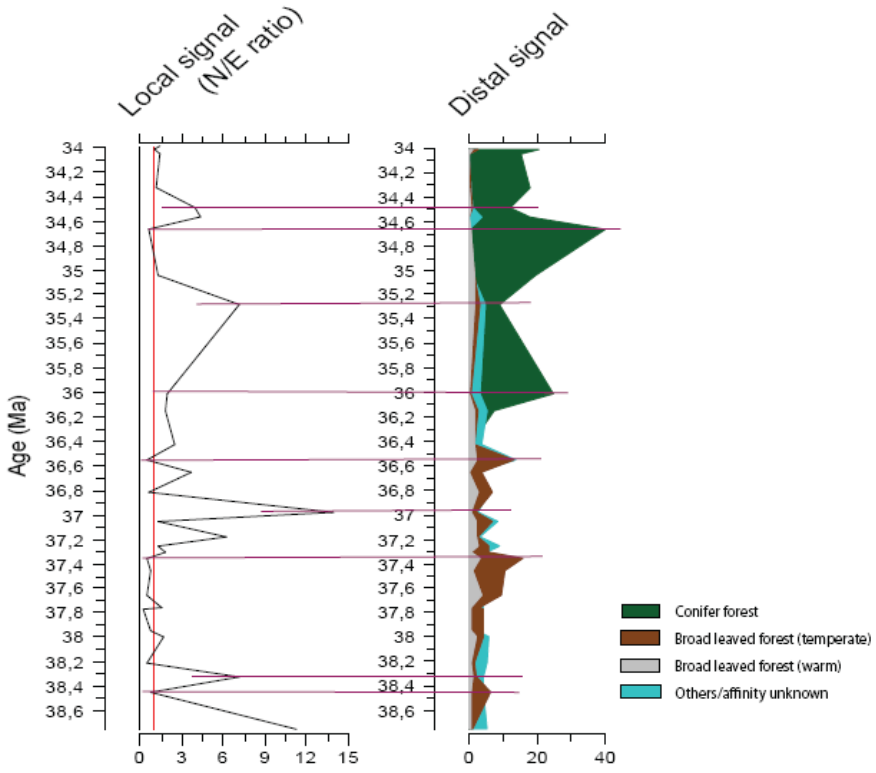


*Figure 14.* The opposite phase relationship between the humidity of the palaeobasin (N/E ratio) and the distal signal, hence, indirectly the humidity of the surroundings.

# 7. Conclusions

1. The abundance of Ephedra and Nitraria-like pollen indicate arid desert and desert-steppe vegetation in the palaeobasin.
2. The pollen data of this study, suggesting arid conditions, fits in the larger regional picture of China during the Eocene. A broad belt of aridity stretched across China from west to east during the Paleogene.
3. Ephedra and Nitraria alternate suggesting fluctuations between deserted and slightly more (humid) conditions.
4. The Nitraria domination is typical for the Eocene of China and is not comparable to Neogene - Present palynological spectra where Chenopodiaceae and Artemisia dominate.
5. Broadleaved forest taxa are common below 36 Ma.
6. Conifers appear and dominate from 36 Ma onwards.
7. The conifers and broadleaved forest taxa suggest a developing mountain belt in the periphery of the depositional environment. This mountain formation is likely to be related to the onset of Tibetan Plateau uplift.
8. Structural and tectonic data supports the hypothesis of early uplift during the Late Eocene.
9. The climatic cooling at the E-O boundary is possibly a consequence of early Plateau formation.
10. Different hypotheses have been formed to explain the fluctuations in the local and distal signals.
11. Both signals have been affected by the interplay of climate changes and tectonics.
12. Higher resolution data and data over a longer time period are needed to say something more viable about the forcing factors and environmental changes.

# 8. Further work

## 8.1 Eocene-Oligocene transition

The samples from this study are dated from 33,97-38,75 Ma, covering the Late Eocene period. The youngest just only coincides with the beginning of the Eocene-Oligocene transition, 33,5-34 million years ago. Therefore palynoflora results of this Eocene-Oligocene transition are beyond the scope of this study.

Time boundaries between two periods are often based on floral changes. Therefore it would be interesting to study the palynofloral changes across the Eocene-Oligocene transition. The study of Dupont-Nivet et al. (2008) contains results of three samples in the Eocene-Oligocene transition, two from the Shuiwan section (at 33,8 Ma and 33,98 Ma), one from the Xiejia section (at 33,3 Ma), ~12 km south from the Shuiwan section. These results are combined with the results of this study; figures 15 and 16 show diagrams of different vegetation types and all taxa, respectively, through the EOT. It should be noted that ages had to be extrapolated, and therefore are not very reliable.

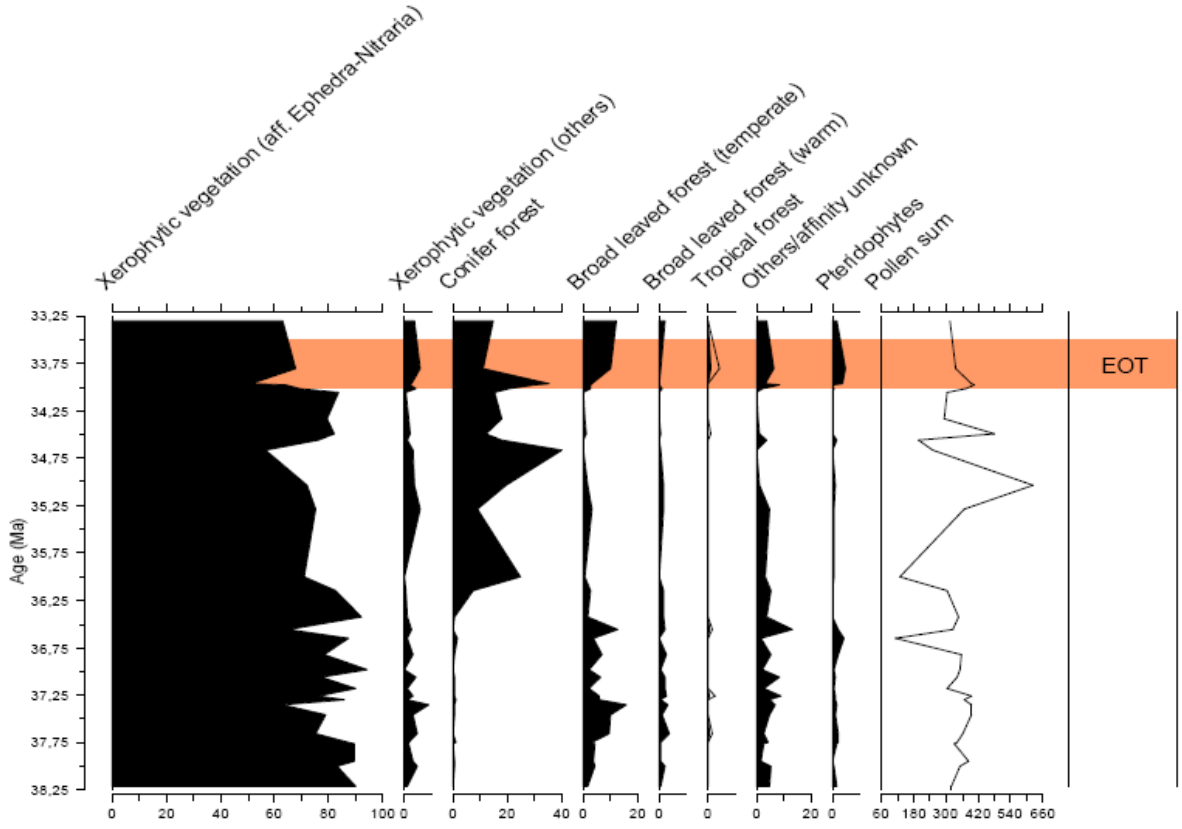


*Figure 15. Pollen diagram of different vegetation types. Data at 33,3 Ma (Xiejia section) , 33,8 Ma and 33,98 are from the study of Dupont-Nivet et al. (2008).*

Figure 15 shows that conifers peak at the beginning of the EOT and then decrease. At the level of decrease of conifers, broad leaved forest taxa, tropical forest taxa, other angiosperm taxa and pteridophytes start significantly to increase. Looking at figure 16 it can be seen that the increase of the broad leaved forest vegetation types highly depends on the increase of Fagaceae and

*Quercoidites (*3c). The amplification of the other angiosperms group is mainly caused by the increase of the *Psilatricolporites.* The increase of pteridophytes mainly depends on the increase of *Lycopodiumsporites*.

As a suggestion for further work these palynofloral changes at the Eocene-Oligocene transition should be studied in greater detail. Higher resolution data of this boundary should be obtained and studied, although this is difficult because due to the aridification in the area around the EOT gypsum beds, containing pollen, disappear. The outcomes should be compared to other Eocene-Oligocene pollen records in China and globally.

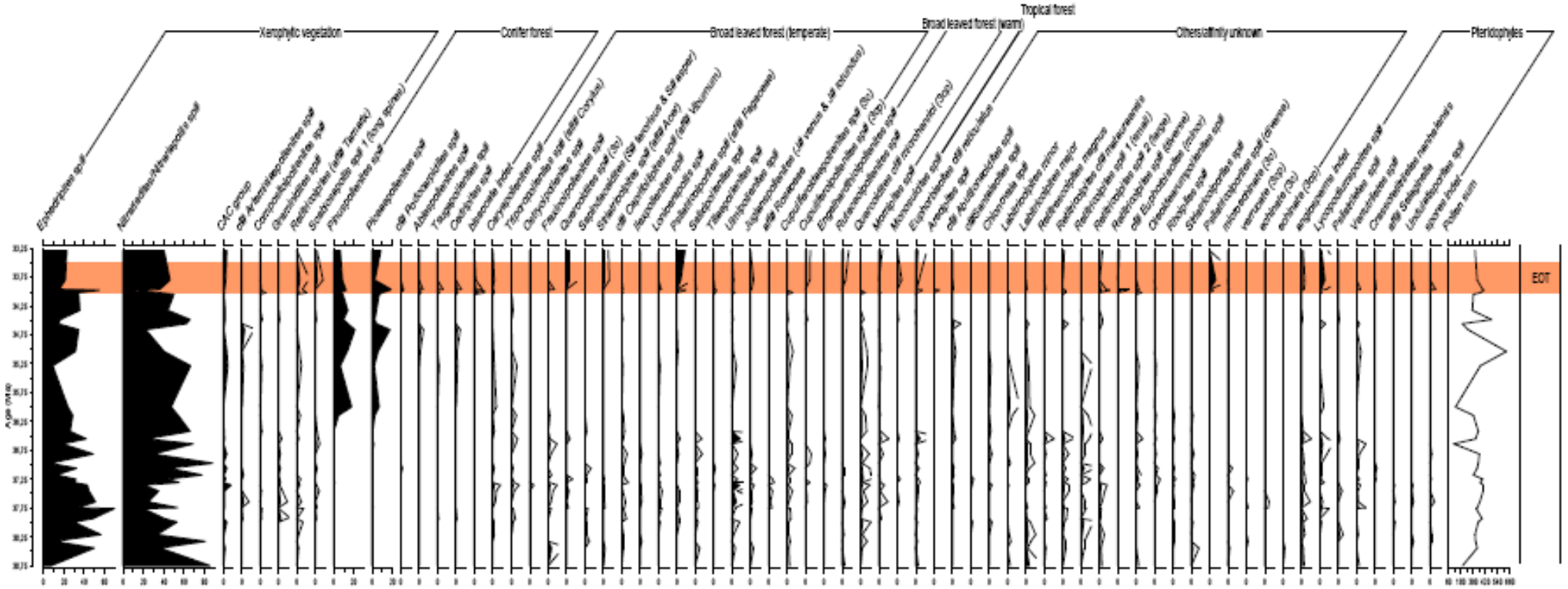


*Figure 16. Pollen diagram of all taxa (magnification by 5 is denoted for the less abundant taxa). Data at 33,3 Ma (Xiejia section) , 33,8 Ma and 33,98 are from the study of Dupont-Nivet et al. (2008).*

## 8.2 Climatic quantification

Variations in climate can be reconstructed via qualitative assessment of pollen percentages, analysis of pollen ratios, application of the biome reconstruction method, and the use of pollen–climate transfer functions. Using modern pollen-climate relationships is a useful tool for quantitative reconstructions of temperature and precipitation (Herzschuh et al., 2009)

Since climatic quantification would be an interesting next step, the following is a synthesis of articles which describe different methods of temperature and precipitation reconstructions.

*Scatter diagrams*

Strong relationships between precipitation, temperature and certain pollen types can be displayed in scatter diagrams. Scatter diagrams reveal pronounced linearities for some pollen types and non-linearities for others in the relationships. The linear relationships generally exist between precipitation and arboreal pollen types as well as some non-arboreal pollen types. Strong positive correlations are found between July temperature and tree pollen types such as *Pinus, Quercus,* and *Betula* (Shen et al., 2006).

*Climate transfer functions*

To obtain quantitative information on precipitation changes, pollen–climate transfer functions can be applied to fossil pollen spectra. Transfer functions are built by using the inverse linear (IL) regression and weighted averaging partial least squares (WA-PLS) regression methods. Birks (1995) provided a detailed description of transfer function methodology and a critical discussion of general theory, assumptions, and techniques used for developing transfer functions (Shen et al., 2006).

*Qualitative assessment of pollen percentages*

To aid the palaeoclimatic interpretation of established pollen zones, a principal component analysis of the pollen data can be performed. This is an ordination technique, displaying the data in a two-dimension PCA correlation biplot (Sun and Zhang, 2008).

Canonical correspondence analysis (CCA) is applied to identify the climate variables that typify the climatic gradients among modern pollen sampling sites and determine the modern pollen–climate relationships. This technique performs a constrained ordination of pollen data in response to two or more climatic variables. The CCA ordination axes are linear combinations of the climatic variables that maximize the dispersion of the pollen taxon scores. CCA is used to reveal the climatic parameters that best reflect the main patterns of variation in the modern pollen rain. These climatic parameters can then be used in the transfer functions (Shen et al., 2006).

*Climatic amplitude method*

The climatic amplitude method is a technique in which the past climate is estimated by transposing the climatic requirements of the maximum number of modern taxa to the fossil data. The results are proposed as temperature intervals and a most likely value corresponding to a weighted mean for three temperature parameters: (1) mean annual temperature; (2) mean temperature of the coldest months and (3) mean temperature of the warmest months (Jiménez-Moreno et al., 2007).

## Acknowledgment

I would like to thank Guillaume Dupont-Nivet and the Utrecht University for making this MSc research possible in the first place. I also would like to thank Guillaume and Carina Hoorn for all their time, patience, fruitful discussions, but mostly their inspirational enthusiasm! Marijke and Hemmo made the fieldtrip in China unforgettable, thank you. Martin Konert of the Free University of Amsterdam is thanked for his laboratory assistance. I am also grateful to Henry Hooghiemstra to make it possible to work at the University of Amsterdam. Special thanks to Jan van Arkel for the beautiful pollen pictures and plates he made. Thanks to all my family and friends, in particular to Willem, although making fun of the pollen subject, for their support.

# References


Birks, H.J.B., 1995, Quantitative palaeoenvironmental reconstructions, *in* Maddy, D., and Brew, J.S., eds., Statistical modelling of Quaternary Science Data.Technical Guide, Volume 5: Cambridge, Quaternary Research Association, p. 161-254.

Boughalleb, F., Denden, M., and Ben Tiba, B., 2009, Anatomical changes induced by increasing NaCl salinity in three fodder shrubs, Nitraria retusa, Atriplex halimus and Medicago arborea: Acta Physiol Plant, v. 31, p. 947-960.

Cour, P., Zheng, Z., Duzer, D., Calleja, M., and Yao, Z., 1999, Vegetational and climatic significance of modern pollen rain in northwestern Tibet: Review of Palaeobotany and Palynology, v. 104, p. 183-204.

Dai, S., Fang, X., Dupont-Nivet, G., Song, C., Gao, J., Krijgsman, W., Langereis, C., and Zhang, W., 2006, Magnetostratigraphy of Cenozoic sediments from the Xining Basin: Tectonic implications for the northeastern Tibetan Plateau: Journal of Geophysical Research, v. 111.

Dupont-Nivet, G., Hoorn, C., and Konert, M., 2008, Tibetan uplift prior to the Eocene-Oligocene climate transition: evidence from pollen analysis of the Xining Basin: Geology.

—, 2009, Erratum: Tibetan uplift prior to the Eocene-Oligocene climate transition: evidence from pollen analysis of the Xining Basin: Geology, v. 37.

Dupont-Nivet, G., Krijgsman, W., Langereis, C., Abels, H.A., Dai, S., and Fang, X., 2007, Tibetan plateau aridification linked to global cooling at the Eocene-Oligocene transition: Nature, v. 445, p. 635-638.

Ehrmann, W., 1998, Implications of late Eocene to early Miocene clay mineral assemblages in McMurdo Sound (Ross Sea, Antarctica) on paleoclimate and ice dynamics: Palaeogeography, Palaeoclimatology, Palaeoecology, v. 139, p. 213-231.

Eldrett, J.S., Greenwood, D.R., Harding, I.C., and Huber, M., 2009, Increased seasonality through the Eocene to Oligocene transition in northern high latitudes: Nature, v. 459, p. 969-973.

Fauquette, S., Suc, J.-P., Bertini, A., Popescu, S.-M., Warny, S., Bachiri Taoufiq, N., Perez Villa, M.-J., Chikhi, H., Feddi, N., Subally, D., Clauzon, G., and Ferrier, J., 2006, How much did climate force the Messinian salinity crisis? Quantified climatic conditions from pollen records in the Mediterranean region: Palaeogeography, Palaeoclimatology, Palaeoecology, v. 238, p. 281-301.

Gao, R., Zhu, Z., Zheng, G., and Zhao, C., 2000, Palynology of petroliferous basins in China: Beijing, Petroleum Industry Press.

Garzione, C.N., 2008, Surface uplift of Tibet and Cenozoic global cooling: Geology, v. 36, p. 1003-1004.

Grimm, E.C., 1987, CONISS: a fortran 77 program for stratigraphically constrained cluster analysisby the method of of incremental sum of squares: Computers & Geosciences, v. 13, p. 13-35.

Hattenschwiler, S., Handa, I.T., Egli, L., Asshoff, R., Ammann, W., and Korner, C., 2002, Atmospheric CO2 enrichment of alpine treeline conifers: New Phytologist, v. 156, p. 363-375.

Herzschuh, U., Kramer, A., Mischke, S., and Zhang, C., 2009, Quantitative climate and vegetationsince the late glacial on the northeastern Tibetan Plateau deduced from Koucha lake pollen spectra: Quaternary Research, v. 71, p. 162-171.

Herzschuh, U., Kurschner, H., Batterbee, R., and Holmes, J., 2006a, Desert plant pollen production and a 160-yera record of vegetation and climate change Veget Hist Archaeobot, v. 15, p. 181-190.

Herzschuh, U., Kurschner, H., and Ma, Y., 2003, The surface pollen and relative pollen production of the desert vegetation of the Alashan Plateau, western Inner Mongolia: Chinese Science Bulletin, v. 48, p. 1488-1493.

Herzschuh, U., Winter, K., Wünnemann, B., and Li, S., 2006b, A general cooling trend on the central Tibetan Plateau throughout the Holocene recorded by the Lake Zigetang pollen spectra: Quaternary International, v. 154-155, p. 113-121.
Horowitz, A., 1992, Palynology of arid lands: Amsterdam, Elsevier Science Publisher B.V.
Horton, B.K., Dupont-Nivet, G., Zhou, J., Waanders, G.L., Butler, R.F., and Wang, J., 2004, Mesozoic-Cenozoic evolution of the Xining-Minhe and Dangchang basins, northeastern Tibetan Plateau: Magnetostratigraphic and biostratigraphic results: Journal of Geophysical Research, v. 109.
Housman, D.C., Naumberg, E., Huxman, T.E., Charlet, T.N., Nowak, R.S., and Smith, S.D., 2006, Increases in Desert Shrub Productivity under Elevated Carbon Dioxide Vary with Water Availability: Ecosystems, v. 9, p. 374-385.
Huntley, B., and Webb, T., 1988, Vegetation history, Handbook of vegetation science, Volume 7: Dordrecht, Kluwer Academic, p. 803.
Jacobson, G.L., 1988, Ancient permanent plots: sampling in paleovegetational studies, *in* Huntley, B., and Webb, T., eds., Vegetation history, Kluwer, p. 3-16.
Jiang, H., and Ding, Z., 2008, A 20 Ma pollen record of East-Asian summer monsoon evolution from Guyuan, Nigxia, China: Palaeogeography, Palaeoclimatology, Palaeoecology, v. 265, p. 30-38.
Jiménez-Moreno, G., Fauquette, S., Suc, J., and Aziz, H.A., 2007, Early Miocene repetitive vegetation and climatic changes in the lacustrine deposits of the Rubielos de Mora Basin (Teruel, NE Spain): Palaeogeography, Palaeoclimatology, Palaeoecology, v. 250, p. 101-113.
Li, J., and Zhang, Y., 2000, Paleogene arid climatic process in China, Palynofloras and Palynomorphs of China: Hefei, Press of University of Science and Technology of China, p. 106-119.
Li, Y., Mingkui, C., and Kerang, L., 2006, Climate-induced changes in the vegetation pattern of China in the 21st century: Ecological Research, v. 21, p. 912-919.
Li, Y., Wang, N., Morrill, C., Cheng, H., Long, H., and Zhao, Q., 2009, Environmental change implied by the relationship between pollen assemblages and grain-size in N.W. Chinese lake sediments since the Late Glacial: Review of Paleobotany and Palynology, v. 154, p. 54-64.
Liu, W., Yang, H., Ning, Y., and An, Z., 2007, Contribution of inherent organic carbon to the bulk [delta]13C signal in loess deposits from the arid western Chinese Loess Plateau: Organic Geochemistry, v. 38, p. 1571-1579.
Lu, H., Wu, N., Yang, X., Shen, C., Zhu, L., Wang, L., Li, Q., Xu, D., Tong, G., and Sun, X., 2008, Spatial patterns of *Abies* and *Picea* surface pollen distribution along the elevation gradient in the Qinghai-Tibetan Plateau and Xinjiang, China: Boreas, v. 37, p. 254-262.
Ma, Y., Liu, K., Feng, Z., Sang, Y., Wang, W., and Sun, A., 2008, A survey of modern pollen and vegetation along a south-north transect in Mongolia: Journal of Biogeography, v. 35, p. 1512-1532.
Miao, F., Fang, X., Song, Z., Wu, F., Han, W., Dai, S., and Song, C., 2008, Late Eocene pollen recordsand palaeoenvironmental changes in northern Tibetan Plateau: Science in China Series D: Earthe Sciences, v. 51, p. 1089-1098.
Molnar, P., and England, P., 1990, Late Cenozoic uplift of mountain ranges and global climate change: chicken or egg?: Nature, v. 346, p. 29-34.
Moore, P.D., Webb, J.A., and Collinson, M.E., 1991, Pollen analysis, Blackwell Scientific Publications.
Pearson, P.N., Foster, G.L., and Wade, B.S., 2009, Atmospheric carbon dioxide through the Eocene–Oligocene climate transition: Nature, v. 461, p. 1110-1113.
Prell, W.L., Wang, P., and Blum, P., 1998, Ocean Drilling Program, Leg 184 Scientific Prospectus, SOUTH CHINA SEA.
Ramstein, G., Fluteau, F., Besse, J., and Joussaume, S., 1997, Effect of orogeny, plate motion and land–sea distribution on Eurasian climate change over the past 30 million years: Nature
v. 386, p. 788-795.

Rowley, D.B., and Currie, B.S., 2006, Palaeo-altimetry of the late Eocene to Miocene Lunpola basin, central Tibet: Nature, v. 439, p. 677-681.
Royden, L.H., Burchfiel, B.C., and Hilst, v.d., R.D., 2008, The geological evolution of the Tibetan Plateau: Science, v. 321, p. 1054-1058.
Ruddiman, W.F., 2001, Earth's climate past and future: New York, W.H. Freeman and Company.
Saxe, H., Ellsworth, D.S., and Heath, J., 1998, Tree and Forest Functionating in an Enriched CO2 Atmosphere: New Phytologist, v. 139, p. 395-436.
Shen, C., Liu, K., Tang, L., and Overpeck, J.T., 2006, Quantitative relationships between modern pollen rain and climate in the Tibetan Plateau: Review of Paleobotany and Palynology, v. 140, p. 61-77.
Smith, S.D., Huxman, T.E., Zitzer, S.F., Charlet, T.N., Housman, D.C., Coleman, J.S., Fenstermaker, L.K., Seemann, J.R., and Nowak, R.S., 2000, Elevated CO2 increases productivity and invasive species success in an arid ecosystem: Nature, v. 408.
Song, Z., 2000, On the first occurence and flourish of some fossil angiosperm shrub and herb pollen in China and their significance, Palynofloras and Palynomorphs of China: Hefei, Press of University of Science and Technology of China, p. 138-150.
Sun, J., and Zhang, Z., 2008, Palynological evidence for the Mid-Miocene Climatic Optimum recorded in Cenozoic sediments of the Tian Shan Range, northwestern China: Global and Planetary Change, v. 64, p. 53-68.
Sun, X., and Wang, P., 2005, How old is the Asian monsoon system?-Palaeobotanical records from China: Palaeogeography, Palaeoclimatology, Palaeoecology, v. 222, p. 181-222.
Talbot, M.R., and Allen, P.A., 1996, Lakes, *in* Reading, H.G., ed., Sedimentary Environments: Processes, Facies and Stratigraphy: Oxford, Blackwell Publishing Inc., p. 83-124.
Tapponnier, P., Zhiqin, X., Roger, F., Meyer, B., Arnaud, N., Wittlinger, G., and Jingsui, Y., 2001, Oblique stepwise rise and growth of the Tibet Plateau: Science, v. 294, p. 1671-1677.
Tripati, A., Backman, J., Elderfield, H., and Ferretti, P., 2005, Eocene bipolar glaciation associated with global carbon cycle changes: Nature, v. 436, p. 341-346.
Wang, C., Zhao, X., Liu, Z., Lippert, P.C., Graham, S.A., Coe, R.S., Yi, H., Zhu, L., Liu, S., and Li, Y., 2008a, Constraints on the early uplift history of the Tibetan Plateau: PNAS, v. 105, p. 4987-4992.
Wang, D., Sun, X., Zhao, Y., and He, Z., 1990, Palynoflora from Late Cretaceous to Tertiary in some regions of Qinghai and Xinjiang, The study on the micropaleobotany from Cretaceous-Tertiary of the oil bearing basins in some regions of Qinghai and Xinjiang, China Environmental Science Press, p. 135-179.
Wang, Q., Wyman, D.A., Xu, J., Dong, Y., Vasconcelos, P.M., Pearson, N., Wan, Y., Dong, H., Li, C., Yu, Y., Zhu, T., Feng, X., Zhang, Q., Zi, F., and Chu, Z., 2008b, Eocene melting of subducting continental crust and early uplifting of central Tibet: Evidence from central-western Qiangtang high-K calc-alkaline andesites, dacites and rhyolites: Earth and Planetary Science Letters, v. 272, p. 158-171.
Xi, Y., and Sun, M., 1987, Pollen morphology of *Nitraria* and its geological distribution: Botanical Research (China), v. 2, p. 235-243.
Xi, Y., and Zhang, J., 1991, The comparative studies of pollen morphology between *Nitraria* and Meliaceae: Botanical Research (China), v. 5, p. 47-58.
Yin, A., and Harrison, T.M., 2000, Geologic evolution of the Himalayan-Tibetan orogen: Annual Review of Earth and Planetary Sciences, v. 28, p. 211-280.
Yu, G., Chen, X., Ni, J., and Cheddadi, R., 2000, Paleovegetation of China: a pollen data-based synthesisfor the mid-Holocene and last glacial maximum: Journal of Biogeography, v. 27, p. 635-664.
Yu, G., Prentice, I.C., Harrison, S.P., and Sun, X., 1998, Pollen-based biome reconstructions for China at 0 and 6000 years: Journal of Biogeography, v. 25, p. 1055-1069.

Zhang, Z., Wang, H., Guo, Z., and Jiang, D., 2007, Impacts of tectonic changes on the reorganization of the Cenozoic paleoclimatic patterns in China: Earth and Planetary science Letters, v. 257, p. 622-644.

Zhao, Y., and Herzschuh, U., 2009, Modern pollen representation of source vegetation in the Quidam Basin and surrounding mountains, north-eastern Tibetan Plateau: Veget Hist Archaeobot, v. 18, p. 245-260.

# Appendices

## Appendix 1 - Pollen references

**Pollen references following Jansonius' Genera File of Fossil Spores, by C.Hoorn**

**Gymnospermae**

*Ephedripites* group
*Ephedripites* subgen. *Spiralipites* Krutzsch 1970
*Ephedripites* subgen. *Dystachyapites* Krutzsch 1961

*Abiespollenites* Thiergart in Raatz (1937) 1938
(in: Abhandl., Presuss. Geol. Landesanst., n.s., H. 138, p. 15-16)
*Cedripites* Wodehouse 1933
(in: Bull. Torrey. Bot. Club, v. 60, p. 497)
*Pinuspollenites* Raatz 1938ex Potonié 1958
(in: Abhandl., Presuss. Geol. Landesanst., n.s., H. 138, p. 15-16)
*Piceaepollenites* Potonié 1931
(in: Sitz.-Ber. Gesellsch. Naturf. Freunde, Jahrg. 1931, no. 1-3, p. 28)
*Podocarpidites* Cookson ex Couper 1953
(in: New Zealand Geol. Surv., Paleontol. Bull. 22, p.35)
cf. *Podocarpidites* sp. Cathaya?
*Rugubivesiculites* Pierce 1961
*Rugubivesiculites* sp.
*Tsugapollenites* Raatz 1937, 1938
(in: Abh. Preuss. Geol. L.-A., n.s., H. 183, p. 15)
Check

**Angiospermae**

**Monocolpate**
*Arecipites* Wodehouse 1933
(in: Bull. Torrey. Bot. Club, v. 60, p. 497)
cf. *Arecipites* sp.
*Liliacidites* Couper 1953
(in: New Zealand Geol. Surv., Paleon. Bull. 22, p. 56)
*Monosulcites*
*Spinozonocolpites*

**Monoporate**
*Graminidites* Cookson ex Potonié 1960
(in: 1947 B.A.N.Z.A.R.E., Reps, ser. A, v.2, pt. 8, p. 134; 1960 Synopsis III, p. 111)

**Diporate**
reticulate (2p)
(in angios indet)

**Triporate**
*Abutilonacidites* Guan Xue-ting & Zheng Ya-hui 1989

( in: Cenozoic-Mesozoic Paleontology and stratigraphy of East China. Series 4. Researches on Late Cenozoic Palynology of the Bohai Sea. Edited by by Design and Research Institute of Bohai Oil
Corporation of CNOOC & Nanjing Institute of Geology and Paleontology, Academia Sinica. Nanjing Univ. Press; Engl. Translation p. 124)
cf. *Abutilonacidites* sp. (aff. *Abutilon)* (smaller than *Abutilonacidites*)

*Betulaceoipollenites* Potonié 1951 ex Potonié 1960
(in: 1951 Palaeontographica, Bd. 91, Abt. B, p. 150; pl. 20, fig. 43; 1960, Synopsis III, p. 114)
*Betulaceoipollenites* sp. (aff. *Betula*)

*Caryapollenites* Raatz (1937) 1938 ex Potonié 1960
(in: Abh. Preuss. Geol. L.-A., 1937, n.s., H. 183, p. 19; Synopsis III, p. 123)
*Caryapollenites* sp.

*Carpinipites* Srivastava 1966
(in: Pollen et Spores, v. 8, no. 3, p. 530)

*Engelhardthioipollenites* Potonié 1951 ex Potonié 1960
(in: Palaeontographica, Bd. 91, Abt. B, p. 145; also pl. 20, fig. 34-38, 1951)
*Engelhardthioipollenites* sp. (aff. *Engelhardtia*)

*Momipites* Wodehouse 1933
(in: Bull. Torrey. Bot. Club, v. 60, p. 497)
*Momipites* sp.

*Triporopollenites* Pflug & Thomson in Thomson & Pflug 1953
(in: Pflug 1952, Paläont. Z., Bd. 26 (nomen nudum); Palaeontographica, Bd. 94, Abt. B, p. 82)
*Triporopollenites* sp. (aff. *Corylus*)

*Ostryoipollenites* Potonié 1951 ex 1960
(in: Palaeontographica, Abt. B, Bd. 91, pl. 20, fig. 46 (nome nudum); 1960: Synopsis III, p. 116 (diagnosis).
*Ostryoipollenites* sp. (aff. *Ostrya*)

cf. *Santalacites* (aff. *Santalum* ) Stelmak 1960 in Povroskaya & Stelmak (in: Atlas; Povroskaya, I.M. & n.K. Stelmak (eds); Leningrad, Trudy VSEGEI, n. Ser., tom 30, p. 225-26)

or Santalaceaepites (aff. *Exocarpus*) or Zonorapollis??

microechinate (3p)

**Tricolpate**

cf. *Artemisiaepollenites*

*Chlonovaia* sp. Elsik 1975
(in: Pollen et Spores, v. 16, p. 528)

*Cupuliferoidaepollenites* Potonié, Thomson & Thiergart 1950 ex Potonié 1960
(in: 1950 geol. Jahrb., Bd. 65, p. 55, 66; 1960 Beih. Geol. Jahrb. Jahrb., H. 39, p. 92)
*Cupuliferoidaepollenites* sp. (3c)

*Elaeagnacites* sp. Ke and Shi 1978
(in: Early Tertiary spores and pollen grains from the coastal region of Bohai. Science. Publ., Beijing, #13031.648; p.131)

*Fraxinoipollenites* Potonié 1951 (Wien) ex Potonié 1960
(in: 195, Mikroskopie, Bd. 6, p. 277; 1960, Beih. Geol. Jahrb., H. 39, p. 94)
*Fraxinoipollenites* sp. (includes R3c type type 4a)

*Labitricolpites* Ke & Shi 1978
(in: Early Tertiary spores and pollen grains from the coastal region of Bohai. Science. Publ., Beijing, #942.13-13; Centr. Catalogue # 13031.648, p. 143)

*Labitricolpites major*
*Labitricolpites minor*
*Lytraidites* Yu Jingxian, Guo Zhenying & Mao Shaozhi 1983
(in: Chinese Acad. Geol. Sci.; Prof. Pap. of Stratigraphy and Palaeontology, no. 10, p. 49)
cf. *Lytraidites* sp.
*Plicapollis* Pflug 1953
(in: Palaeontographica, Abt. B, Bd. 95, p. 97)
*Quercoidites* (3c/deciduous)
*Retitrescolpites* Sah 1967 (Dec.)
(in: Mus. Roy. Afrique Centr., Tervuren; Ann., ser. In 8°, Sci. Geol., no. 57, p.56)
*Retitrescolpites magnus*
*Retibrevitricolpites*
*Retitricolpites*
*Retitricolpites* cf. *matauraensis* (type 6)
*Retitricolpites* aff. *Tamarix*
*Retitricolpites* (small) (type 4c)
*Retitricolpites* (large) (type 25&37)

*Sapindaceidites* Sun & Zhang 1979 in Sun, Zhang & Hou
(in: Acta Bot. Sinica, v. 21, p. 290)
*Sapindaceidites terorisus* (aff. Elaeagnaceae?)
*Sapindaceidites asper* (aff. Elaeagnaceae?)

*Scabiosapollis* Sung Tzechen & Zheng Yahui in Li Manying, Sung Tzechen & Li Zaiping 1978
(in: Nanjing Institute of Geology and Paleontology, Academia Sinica, Mem., no. 9, p. 37)

*Scabiosapollis* sp. 1 (long spines)
*Scabiosapollis* sp. 2 (short spines)
*Scabiosapollis minutes*

*Striatricolpites* (aff. Acer)

microechinate (3c)
verrucate (3c)
echinate (3c)

**Tricolporate**
cf. *Artemisiaepollenites*
*Caprifoliipites* Wodehouse 1933
(in: Bull. Torrey. Bot. Club, v. 60, p. 518) is tricolpate furrows long and pointed pore rims
cf. *Caprifoliipites* (aff. *Viburnum*)
*Compositoipollenites* Potonié 1951 ex Potonié 1960
(in: Synopsis III, p. 105)

*Cupuliferoipollenites* Potonié 1951 ex Potonié 1960
(in: Palaeontographica, Bd. 91, Abt. B, p. 145; 1960 Synopsis III, p. 98)
*Cupuliferoipollenites* sp. (3cp, aff. *Castanea*)
*Euphorbiacites* (Zaklinskaja 1956) ex Li, Sung & Li 1978 Sung & Li in Sung, Lee & Li 1976
(in: Mesozoic fossils from Yunnan; fasc. 1. Nanjing Institute of Geology and Paleontology; Academia Sinica, Science Press, Peking: p. 50, textfig.3)

*Euphorbiacites* cf. *reticulatus* (3cp) Li, Sung & Li
*Euphorbiacites* cf. *reticulatus* (3c)
cf. *Euphorbiacites minor* Zhang et Zhan 1991
cf. *Euphorbiacites* sp.
*Ilexpollenites* Thiergart 1937 ex Potonié 1960
(in: Synopsis III, p. 99)
*Ilexpollenites sp.*
*Lonicerapollis* Krutzsch 1962[a]
(in: Geologie, Jahrg. 11, no.3, p. 274)
*Lonicerapollis* sp.
*Margocolporites*

**Nitrariadites/Nitraripollis Group**

*Nitrariadites* Zhu & Xi Ping in Zhu Zunghao et al. 1985
(in: A research on Tertiary palynology from the Qaidam Basin, Qinghai Province. Edited by Research Inst. Explor. Devel., Qinhai Petr. Adm.; Nanjing Institute of Geology and Paleontology, Academia Sinica, Petr. Industry Press; p. 196 (Engl. Transl. p. 224-5).
*Nitrariadites* sp. ('microreticulate')
*Nitrariadites* sp. ('striate')
*Nitrariadites* sp. ('pseudopsilate')

*Nitraripollis* Xi Yizhen 7 Sun Mengrong 1987
(in: Botanical Research, 1987, no. 2, p. 239; Engl. Transl. p. 243)
*Povrovsjkaya* Boitsova in Boitsova et al. 1979
(in: VSEGUI, Trudy, nov. ser., tom 267, p. 55)
cf. *Qinghaipollis* Zhu Zunghao in Zhu et al. 1985
(in: A research on Tertiary palynology from the Qaidam Basin, Qinghai Province. Edited by Research Inst. Explor. Devel., Qinhai Petr. Adm.; Nanjing Institute of Geology and Paleontology, Academia Sinica, Petr. Industry Press; p. 196 (Engl. Transl. p. 225)

*Oleoidearumpollenites* Nagy 1969
(in: Ann. Inst. Geol. Publ. Hungarici, v. 52, P. 429)
Is cp, baculae 2-4u. differs from Capri in smaller baculae
*Psilatricolporites* (aff. Fagaceae)
*Rhoipites* Wodehouse 1933
(in: Bull. Torrey. Bot. Club, v. 60, p. 513)
*Rhoipites* sp.
*Rutaceoipollenites* He Yue-ming & Sun Xiang-jun 1977
(in: Acta Botot. Sinica, v. 19, p.73)
*Rutaceoipollenites* sp.
*Salixipollenites* Srivastava 1967
(Jan.) (in: Pollen et Spores, v. 8, no. 3, p. 529)
*Salixipollenites* sp. (aff. *Salix)*
*Sapotaceoidaepollenites* Thomson & Thiergart 1950 ex Potonié 1960
(in: 1950 geol. Jahrb., Bd. 65, p. 62; 1960 Synopsis III; Beihefte zum Geologischen Jahrbuch, vol. 39, p.109)
*Sapotaceoidaepollenites* sp.
*Striatricolporites* sp. (Type 28) Van der Hammen ex Leidelmeyer 1966 (in: Leidse Geol. Mededel., v.38, p.58)

*Trudopollis* Pflug 1953b
(in: Palaeontographica, Bd. 95, Abt. B, p. 98)
*Trudopollis* sp.
*Tiliaepollenites* Potonié 1931
(in: Jahrb. Preuss. Geol. L.-A., Bd. 52, p.4)
*Tiliaepollenites sp. (*aff. *Tilia)*

*Quercoidites* Potonié, Thomson & Thiergart 1950 ex Potonié 1960
(in: 1950 geol. Jahrb., Bd. 65, p. 54; 1960 Synopsis III; Beihefte zum Geologischen Jahrbuch, vol. 39, p.92)
*Quercoidites* cf. *microhenrici* (3cp/evergreen)

microechinate (3cp aff. Rosaceae)
verrucate (3cp)
aff. Euphorbiaceae (Croton type)

**Stephanoporate**
*Ulmipollenites* Wolff 1935
(in: Arb., Inst. Palaobot., Petrogr. Brennst., Bd. 5, p. 75)

**Stephanocolporate**
*Alnuspollenites*

**Periporate**

Chenopodiaceae-Amarantaceae-Caryophyllaceae Group
*Chenopodipollis* Krutzsch 1966
(in: Geologie, Beiheft 55, p. 35)
*Chenopodipollis* sp. (aff. Chenopodiaceae/Amarantaceae)
*Carophyllidites* Couper 1960 (September)
(in: New Zealand Geol. Surv. Paleont. Bull 32, p. 68)
*Carophyllidites* sp. (aff. Caryophyllaceae)

*Juglanspollenites* Raatz 1939
(in: Abhandl., Presuss. Geol. Landesanst., n.s., H. 138, p. 18)
*Juglanspollenites rotundus*
*Juglanspollenites verus*
*Persicarioipollis* sp. aff. *Persicaria* Krutzsch 1962[a]
(in: Geologie, Jahrg. 11, no.3, p. 282)

**Tetrade**
*Ericipites* Wodehouse 1933
(in: Bull. Torrey. Bot. Club, v. 60, p. 497)
*Ericipites* sp. (aff. Ericaceae)

**Pteridophyta**

**Monolete**
Psilamonoletes

Echimonoletes
Verrumonoletes

**Trilete**

*Brochotriletes* Naumova 1939 ex Ischenko 1952
(1939 Rept. Intern. Geol. Congr., 17 sess., Moscow 1937, v.l., p. 355; 1952 Akad. Nauk SSSR, Inst. Geol. Nauk; Atlas, p. 40)
*Brochotriletes bellus*
*Lycopodiumsporites* Thiergart 1938
Psilatriletes
Verrutriletes
*Crassoretitriletes nanhaiensis*
aff. *Selaginella*
*Undulatisporites* Pflug in Thomson & Pflug 1953
(in: Palaeontographica, Bd. 94, Abt. B, p. 52)
*Undulatisporites sp.*

## Appendix 2 – Vegetation types

**Vegetation types following Yu et al. (2000). Fossil taxa and their nearest living relative(s) (NRL), by C.Hoorn**

**Xerophytic vegetation (Ephedra-Nitraria)**
*Ephedripites* subgen. *Spiralipites*
*Ephedripites* subgen. *Dystachyapites*
*Nitrariadites* sp. ('microreticulate')
*Nitrariadites* sp. ('striate')
*Nitrariadites* sp. ('pseudopsilate')
cf. *Qinghaipollis* sp.

**Xerophytic vegetation (others)**
CAC group: *Chenopodipollis* sp. (Chenopodiaceae/Amarantaceae) and *Caryophyllidites* (Caryophyllaceae)
*Liliacidites* sp.
*Graminidites* sp
cf. *Artemisiaepollenites* sp. (*Artemisia*)
*Compositoipollenites sp.* (Asteraceae)
*Retitricolpites* (*Tamarix)*
*Scabiosapollis* sp. 1 (long spines) (*Scabiosa*)
*Scabiosapollis* sp. 2 (short spines) (*Scabiosa*)

**Conifer forest**
*Abiespollenites* sp. (*Abies*)
*Cedripites* sp. (*Cedrus*)
*Pinuspollenites* sp. (*Pinus*)
*Piceaepollenites* sp. (*Picea*)
cf. *Podocarpidites* sp. (*Podocarpus*)
*Tsugapollenites* sp. (*Tsuga*)

**Broadleaved forest (temperate)**
*Betulaceoipollenites* sp. (*Betula*)
*Caryapollenites* sp. (*Carya*)
*Carpinipites* sp. (*Carpinus*)
*Cupuliferoidaepollenites* sp. (3c) (Cupuliferae)
*Cupuliferoipollenites* sp. (3cp) (Castanea, Cupuliferae)
*Triporopollenites* sp. (*Corylus*)
*Ostryoipollenites(Ostrya)*
*Elaeangnacites* sp. (Elaeagnaceae)
*Fraxinoipollenites* sp.(*Fraxinus*)
*Quercoidites* sp. (3c) (*Quercus*, deciduous)
*Sapindaceidites terorisus* (Elaeagnaceae?)
*Sapindaceidites asper* (Elaeagnaceae?)
*Striatricolpites* sp. (*Acer*)
cf. *Caprifoliipites* sp. (*Viburnum*)
*Ilexpollenites* sp. (*Ilex*)
*Lonicerapollis* sp. (*Lonicera*)
*Psilatricolporites* sp. (Fagaceae)
*Salixipollenites* sp. (*Salix)*
*Tiliaepollenites* sp. (Tiliaceae)
*Ulmipollenites* sp. (Ulmaceae)
*Alnuspollenites* sp. (*Alnus*)
*Juglanspollenites rotundus* (Juglandaceae)
*Juglanspollenites verus* (Juglandaceae)
*Ericipites* sp. (Ericaceae)
Rosaceae (3cp, microechinate)
Euphorbiaceae (*Croton* type)

**Broad-leaved forest (warm)**
*Engelhardthioipollenites* sp. (*Engelhardtia*)
*Momipites* sp. (*Engelhardtia*)
*Rutaceoipollenites* sp. (Rutaceae)
*Quercoidites* cf. *microhenrici* (3cp)(*Quercus*, evergreen)

**Tropical**
cf. *Arecipites* sp.
*Monosulcites* sp.
*Spinozonocolpites* sp.
*Sapotaceoidaepollenites* sp. (Sapotaceae)

**Others/affinity unknown**
cf. *Abutilonacidites* (*Abutilon*)
cf. *Santalacites* (*Santalum*)
*Chlonovaia* sp.
*Labitricolpites major*
*Labitricolpites minor*
cf. *Lytraidites* sp.
*Plicapollis* sp.
*Retitrescolpites magnus*
*Retibrevitricolpites* sp.
*Retitricolpites* cf. *matauraensis*
*Retitricolpites* sp. 1 (small)
*Retitricolpites* sp. 2 (large)
*Scabiosapollis minutus*
*Euphorbiacites* cf. *reticulatus* (3cp) (Tiliaceae?)
*Euphorbiacites* cf. *reticulatus* (3c) (Tiliaceae?)
cf. *Euphorbiacites minor*
cf. *Euphorbiacites* sp.
*Margocolporites* sp.

*Oleoidearumpollenites* sp.
*Rhoipites* sp.
*Striatricolporites* sp.
*Persicarioipollis* sp. (*Persicaria*)
microechinate (3c)
verrucate (3c)
echinate (3c)
microechinate (3p)
microechinate (3p)
verrucate (3cp)
echinate (3cp)
reticulate (2p)
fenestrate
diporate, reticulate

**Pteridophytes**
Diverse monolete types
*Lycopodiumsporites* sp.
*Psilatriletes* sp.
*Verrutriletes* sp.
*Crassoretitriletes nanhaiensis*
*Selaginella*
*Undulatisporites* sp.

## Appendix 3 - Descriptions *Nitraria* group

**Pollen morphology of *Nitraria* and its geological distribution, Xi and Sun (1987), Xi and Zhang (1991), translation by Y. Xu**

***Nitraria***

***N. sibirica*** Pall.

*Diagnosis:* Pollen grain (34.8-41.7)38.3×24.3(22.6-27.8)µm, outline elliptical in lateral view, and gradual sharp in two polar areas; 3-colporate, colpi long, extending to the poles; pores rounded, almost split along the equator, cateyed; exine solid, 3.5 µm in thickness; surface ornamentation fine-reticulate under optical microscope, and striated under scanning microscope.

*Occurrence:* Northeast and Northwest of China; Mongolia; Soviet Union (Russia).

***N. sphaeorocarpa*** Maxim.

*Diagnosis:* Pollen grain (36.5-41.7)38.3×24.3(22.6-26.1)µm, outline elliptical in lateral view, and gradual sharp in two polar areas; 3-colporate, colpi long, extending to the poles; pores slightly transverse long, split along the equator; exine solid, 3.0 µm in thickness; surface ornamentation fine-reticulate or smooth under optical microscope, and striated under scanning microscope.

*Occurrence:* Northeast China and Nei Monggol Province; Mongolia.

***N. roborowskii*** Kom.

*Diagnosis:* Pollen grain (45.4-52.2) 48.7×29.6 (27.8-31.3)µm, outline prolate in lateral view, gradual sharp in one polar and the other flat; 3-colporate, colpi long, extending to the poles; pores rounded; exine solid, 5.2 µm in thickness; surface smooth or fine-reticulate ornamentation under optical microscope, and striated under scanning microscope.

*Occurrence:* Northeast China; Mongolia; Soviet Union (Russia).

***N. tangutorum*** Bobr.

*Diagnosis:* Pollen grain (46.9-53.9) 48.9×29.6 (27.8-31.3)µm, outline prolate in lateral view, gradual sharp in one polar and the other flat; 3-colporate, colpi long, extending to the poles; pores rounded; exine solid, 4.3 µm in thickness; surface faint fine-reticulate ornamentation under optical microscope, and striated under scanning microscope.

*Occurrence:* Northeast China and Nei Monggol Province.

***N. schoberi*** L.

*Diagnosis:* Pollen grain (38.3-45.4) 43.5×27.8 (26.1-29.5)µm, outline elliptical in lateral view; 3-colporate, colpi narrow, extending to the poles; pores transverse long; exine solid, 4.8 µm in

thickness; surface faint fine-reticulate ornamentation under optical microscope, and striated under scanning microscope.

*Occurrence:* Northeast China.

***Nitraripollis***

***Nitraripollis*** Sun Meng-Rong et Xi Yi-zhen gen. nov. (Xi and Sun, 1987)

*Diagnosis:* Pollen grain prolate, outline elliptical or subrounded in lateral view and roundedly triangular in polar view; 3-colporate, colpi long, extending to the poles; pores rounded, rhombic, or wide-elliptical, almost transverse long along the equator, rarely no split; exine solid, 3 layers, foot layer is thicker than tectum and columella, accompanying the thickened zone in two polar areas and along colpi; ornamentation reticulate, or granulate, sometimes smooth.

*Type species:* ***Nitraripollis tungxinensis*** gen. et sp. Nov.

*Remarks:* Differs from *Meliaceoidites* in having more acute polar areas, and a three-layer exine, with distinct thick foot layer.

*Affinity: Nitraria* of Zygophyllaceae.

*Occurrence:* Asia; Tertiary, especially Oligocene.

***N. tungxinensis*** Xi et Sun 1987 (was Meliaceoidites rhomboiporus, Wang 1980)

1982, Meliaceoidites rhomboiporus Wang, Sun Shuying, Plate 2, fossil 1.

*Diagnosis:* Pollen grain 39-47.5×25.3-35 μm, outline elliptical in lateral view, and rounded or gradual sharp in two polar areas; 3-colporate, colpi long, extending to the poles; pores rhombic, almost split along the equator; exine solid, 2.5-3 μm in thickness, 3 layers, foot layer is thicker than tectum and columella, accompanying the thickened zone in two polar areas and along colpi; ornamentation reticulate, or surface coarse.

*Occurrence:* Dingqing Fm., Oligocene, Lunpola Basin, Tibet; Qingshuiying Fm., Oligocene, Tongxin County, Ningxia Province.

***N. rotundiporus*** comb nov. Xi et Sun 1987 (Ke et Shi, 1978)

1978, Meliaceoidites rotundiporus Ke et Shi, Page 126, Plate 23, fossils 8, 9, 19.

1982, Meliaceoidites rotundiporus, Sun Shuying, Plate 2, fossil 3.

*Diagnosis:* Pollen grain 39.1-41.25×25-28.75 μm, outline elliptical in lateral view, and rounded in two polar areas; 3-colporate, colpi long, extending to the poles; pores rounded, almost no split along the equator; exine solid, 2.5-3.75 μm in thickness, 3 layers, foot layer is thicker than tectum and columella, accompanying the thickened zone in two polar areas and along colpi; ornamentation thin-reticulate, or blurry granulate.

*Occurrence:* Dingqing Fm., Oligocene, Lunpola Basin, Tibet; Qingshuiying Fm., Oligocene, Tongxin County, Ningxia Province; Shahejie Fm. And Dongying Fm., Paleogene, Bohai Sea.

***N. major*** Xi et Sun 1987

*Diagnosis:* Pollen grain 48.3-57.5×30-33.75 μm, outline elliptical in lateral view, and rounded in two polar areas, or one sharp and the other wide-planar; 3-colporate, colpi long, extending to the poles; pores rounded, almost no split along the equator; exine solid, 2.5-3.5 μm in thickness, 3 layers, foot layer is thicker than tectum and columella, accompanying the thickened zone in two polar areas; ornamentation blurry thin-reticulate.

*Occurrence:* Dingqing Fm., Oligocene, Lunpola Basin, Tibet; Qingshuiying Fm., Oligocene, Tongxin County, Ningxia Province.

***N. fusiformis*** Xi et Sun 1987

*Diagnosis:* Pollen grain 29-36.8×18-23 μm, outline spindly in lateral view, and sharp in two polar areas, and the polar axis long; 3-colporate, colpi long, extending to the poles; pores rounded, almost split along the equator; exine solid, 2.5 μm in thickness, 3 layers, foot layer is thicker than tectum and columella, accompanying the thickened zone in two polar areas and along colpi; ornamentation blurry granulate.

*Occurrence:* Dingqing Fm., Oligocene, Lunpola Basin, Tibet; Qingshuiying Fm., Oligocene, Tongxin County, Ningxia Province.

***N. ovatus*** Xi et Sun 1987

*Diagnosis:* Pollen grain 28.75-32.2×21.25-23.75 μm, outline wide-ovate in lateral view; 3-colporate, colpi long, extending to the poles; pores transverse long, almost a little split along the equator; exine solid, 2.5-3.5 μm in thickness, 3 layers, foot layer is thicker than tectum and columella, accompanying the thickened zone in two polar areas and along colpi; ornamentation blurry granulate.

*Occurrence:* Dingqing Fm., Oligocene, Lunpola Basin, Tibet; Qingshuiying Fm., Oligocene, Tongxin County, Ningxia Province.

# Appendix 4 - Pollen plates

Photo plates made by C.Hoorn & J. Van Arkel

**Captions for pollen plates**

The reference sample number is indicated after genus name. See bar for scale in microns.

**Plate 1 (fossil taxa)**

1a & b *Ephedripites* sp., type 1 (PSW03)
2 *Ephedripites* sp., type 2 (PSW32)
3 *Ephedripites* sp., type 3 (P387)
4 *Ephedripites* sp., type 4 (PSW32)
5 *Ephedripites* sp., type 5 (P387)
6 *Ephedripites* sp., type 6 (PSW40)
7 *Ephedripites* sp., type 8 (PSW43a)
8 *Piceapollenites* sp. (PSW02)
9 *Rugubivesiculites* sp. (PSW27)
10 *Spinozonocolpites* sp. (PSW 20)
11a & b Diporate, reticulate pollen type (PSW20b)
12 *Caryapollenites* sp. (PSW31)
13 *Momipites* sp. (P387)
14 *Engelhardthioipollenites* sp. (PSW31b)
15 *Triporopollenites* sp. (PSW30a)
16 *Santalaceaepites* sp. (P11)
17 *Juglanspollenites rotundus* (P387)
18 *Juglanspollenites verus* (PSW29)
19 *Ulmipollenites* sp. (PSW387)
20 *Carophyllidites* sp. (PSW29)
21 *Carophyllidites* sp. (PSW31)
22 *Chenopodipollis* sp. (PSW31b)
23 *Abutiloncidites* sp. (PSW 28)
24 *Chlonovaia* sp. (PSW24)
25 *Scabiosapollis* sp., type 1 (P387a)
26 *Scabiosapollis* sp., type 1 (PSW31b)
27 a & b *Scabiosapollis minutus* (PSW02)
28 *Fraxinoipollenites* sp. (P12)
29 a & b *Fraxinoipollenites* sp. (P12)
30 *Retitricolpites* sp., type 25-37 (P387)
31a & b *Retitricolpites* sp., type 4c (PSW 29a)
32 *Retitricolpites* sp., type 4a (PSW 02)
33 a & b *Retitricolpites* sp., type 4b aff. Tamarix (PSW 02
34 a & b *Retitricolpites* sp., type 4b aff. Tamarix (PSW 34)
35 *Retitricolpites mataurensis* (PSW 44)
36 *Retitrescolpites* sp. (P11)
37 *Retitrescolpites* sp. (PSW 25)
38 a & b *Plicapollis* sp. (PSW 29)
39 a & b *Cupuliferoidaepollenites* sp. (3c) (PSW 30a)
40 a & b *Striatricolpites* sp., aff. Acer (P384)
41 *Sapindaceidites* sp., type 1(P387)
42 *Sapindaceidites* sp., type 2 (P387)
43 *Sapindaceidites tetrorisus* (P12)
44 a & b *Retibrevitricolpites* sp. (PSW 387)
45 Tricolpate, microechinate pollen type (PSW02)

**Plate 2**

1a & b *Labitricolpites minor* (PSW03)
2 *Labitricolpites major* (PSW27)
3 *Labitricolpites minor* (P379)
4 a&b *Nitraripollis* sp., type 3 (PSW02)
5 a&b *Nitraripollis* sp., type 2 (PSW31)
6 a&b *Nitraripollis* sp., type 5 (PSW32)
7 a, b & c *Nitraripollis* sp., type 1 (P385)
8 a, b & c *Nitraripollis* sp., type 5 (PSW02)
9 a&b *Nitraripollis* sp., type 5 (PSW27b)
10 *Nitraripollis* sp., type 5 (PSW 26)
11 *Nitraripollis* sp. corroded (PSW30a)
12 a, b & c *Nitraripollis* sp., type 4 (PSW27b)
13 *Nitraripollis* sp., type 9 (PSW27b)
14 a&b *Nitraripollis* sp. (PSW28)
15 a&b *Nitraripollis* sp., type 7 (PSW26)
16 a&b *Nitraripollis* sp., type 2 (PSW30)
17 a, b & c *Nitraripollis* sp., type 8 (P387)
18 a&b *Nitraripollis* sp., type 8 (PSW27b)
19 a, b & c *Euphorbiacites* sp., type 1 (P12)
20 *Euphorbiacites* sp., type 2 (PSW45b)
21 a & b *Euphorbiacites* sp., type 3 (P387)
22 a, b & c *Euphorbiacites* sp., type 3 (PSW27b)
23 a & b *Retitricolporites* sp., type 1 (was type 33) (PSW 29a)
24 a & b *Cupuliferoipollenites* sp. (3cp) (PSW26)
25 a & b *Quercoidites* sp. (evergreen type) (PSW31b)

**Plate 3**

1 a & b Microechinate, tricolporate pollen type, aff. Rosaceae (PSW34a)
2 a, b & c *Retitricolporites* sp., type 2, equatorial view (PSW20)
3 a, b & c *Retitricolporites* sp., type 2, polar view (PSW20)
4 a, b & c *Striatricolporites* sp. (PSW28)
5 *Tiliaepollenites* sp. (PSW02)
6 *Oleoidearumpollenites* sp. (PSW31b)
7 *Oleoidearumpollenites* sp. (PSW02)
8 a & b *Oleoidearumpollenites* sp. (PSW32)
9 a & b *Salixipollenites* sp. (PSW20)
10 *Ilexpollenites* sp. (PSW 34)
11 *Rutaceoipollenites* sp. (P387)
12 a & b *Caprifolipites* sp. (PSW03)
13 *Caprifolipites* sp. (PSW02)
14 *Lonicerapollis* sp. spec. 1 (PSW32)
15 *Lonicerapollis* sp. spec2 (PSW28)
16 a & b *Ericipites* sp. (PSW33)
17 *Undulatisporites* sp. (PSW387)
18 Echinate, trilete spore aff. Selaginella (PSW387)
19 a & b *Crassoretitriletes nanhaiensis* (PSW27b)
20 a & b. *Verrutriletes* sp. (PSW29)
21 *Brochotriletes bellus* (P12)
22-25 *Glomus*, contamination

**Plate 4 (the extant taxon Nitraria; slides provided by F. Schlutz)**

1 a & b *Nitraria tangutorum*
2 a & b *N. tangutorum*
3 a & b *N. tangutorum* (polar view)
4 a & b *Nitraria sphaerocarpa* (sample Kashan 2000)
5 a & b *N. sphaerocarpa* (polar view) (sample Kashan 2000)
6 a, b & c *N. sphaerocarpa*
7 a & b *N. sphaerocarpa*
8 a, b & c *Nitraria sibirica* (sample from west Mongolia, HAL 40706)
9 a, b & c *N. sibirica* (sample from west Mongolia, HAL 40706)
10 a & b *N. sibirica* (polar view) (sample from west Mongolia, HAL 40706)
11 a & b *N. sibirica*
12 a & b *N. sibirica* (polar view)
13 a, b & c *Nitraria roborowskii*
14 a, b & c *N. roborowskii*
15 a & b *Nitraria schoberi* (sample from Iran courtesy of Mortreza Djamali)
16 a, b, c & d *N. schoberi* (sample from Iran courtesy of Mortreza Djamali)

**Pollen plate 1**

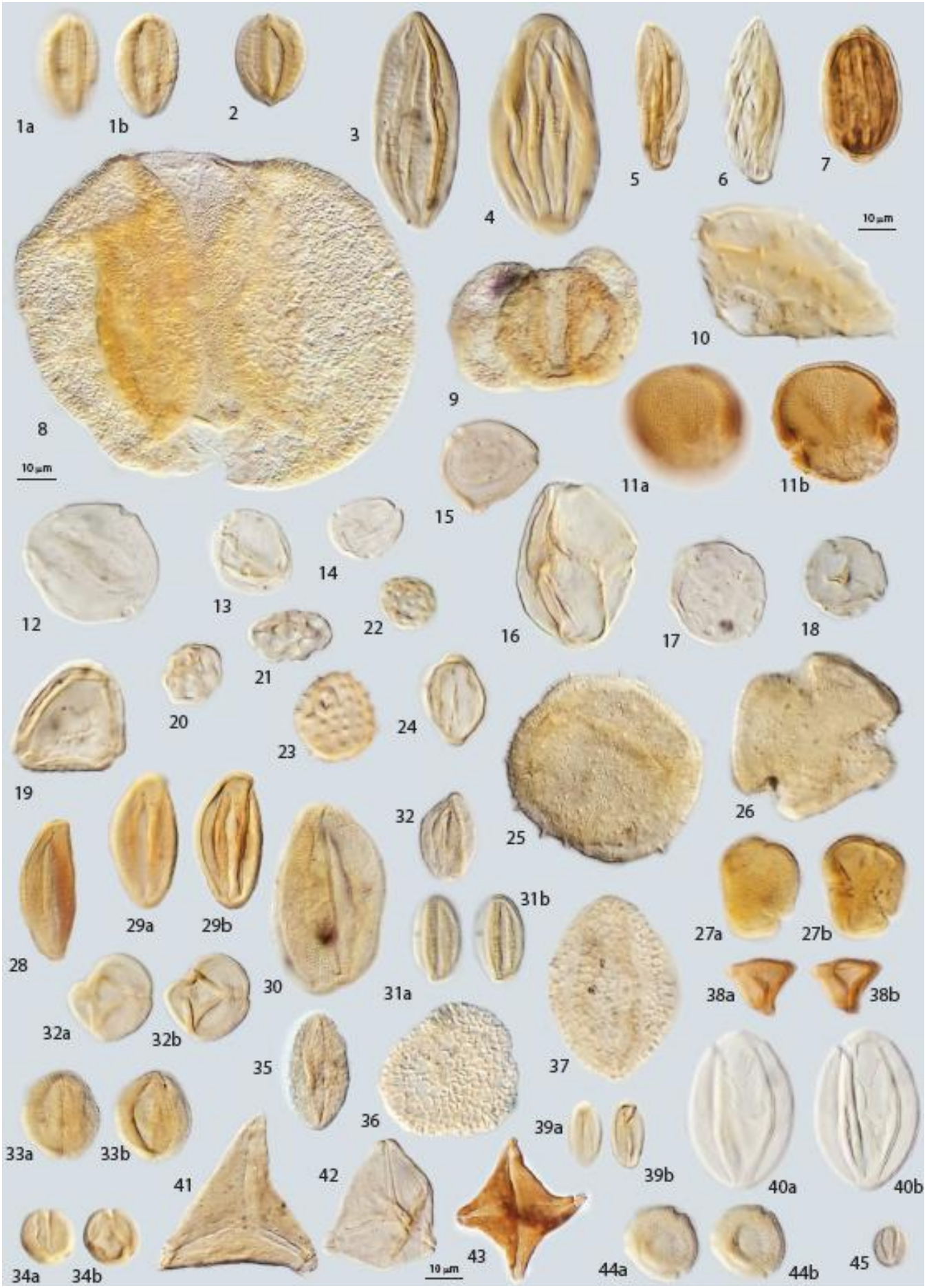

**Pollen plate 2**

**Pollen plate 3**

**Pollen plate 4**